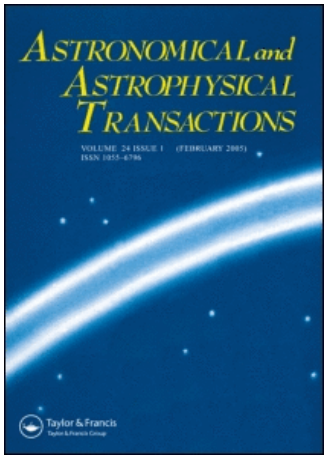

Astronomical & Astrophysical Transactions
The Journal of the Eurasian Astronomical Society
Publication details, including instructions for authors and subscription information:
http://www.informaworld.com/smpp/title~content=t713453505

The elastic energy of rotational and lunisolar tides and their role in the Earth's seismic activity

Yu. V. Barkin [ab]; J. M. Ferrandiz [b]; M. Garcia Ferrandez [b]; J. F. Navarro [b]
[a] Sternberg Astronomical Institute, Universitetskii Prospekt 13, Moscow, Russia
[b] Department of Applied Mathematics, Alicante University, Alicante, Spain

Online Publication Date: 01 August 2007
To cite this Article: Barkin, Yu. V., Ferrandiz, J. M., Ferrandez, M. Garcia and Navarro, J. F. (2007) 'The elastic energy of rotational and lunisolar tides and their role in the Earth's seismic activity', Astronomical & Astrophysical Transactions, 26:4, 163 - 198
To link to this article: DOI: 10.1080/10556790601017224
URL: http://dx.doi.org/10.1080/10556790601017224

Astronomical and Astrophysical Transactions
Vol. 26, Nos. 4–5, August–October 2007, 163–198

The elastic energy of rotational and lunisolar tides and their role in the Earth's seismic activity

YU. V. BARKIN*†‡, J. M. FERRANDIZ‡, M. GARCIA FERRANDEZ‡ and J. F. NAVARRO‡

†Sternberg Astronomical Institute, Universitetskii Prospekt 13, Moscow 119899, Russia
‡Alicante University, Department of Applied Mathematics, Alicante, Spain

(Received 14 September 2006)

An analytical expression for the elastic energy of the planet tidal deformations induced by external celestial bodies and by the rotational motion of the planet has been obtained. It was shown that the elastic energy is not the additive sum of the elastic energies of rotation and the corresponding planet–perturbing body pairs but contains additional terms of mutual character. Previously we have obtained a formula for the elastic energy of superposition of the lunisolar tides which also contains additional terms of mutual character caused by the mutual influence of the Moon and the Sun. In this paper we have obtained new mutual terms caused by the combination of the rotational deformations of the planet and by lunisolar tides. These additional terms are more significant and determine the main variations in the global tension state of the Earth. With various degrees of detail, we have looked at the variations in this energy in the last few decades, and also for a hundred years into the future. The peak excited conditions of the Earth and the condition of the active decrease in the elastic energy were determined on a timescale from 100 to 2100. The correlation of extreme variations in the elastic tidal energy of the Earth with large earthquakes has been studied.

Keywords: Rotational tide; Lunisolar tides; Superposition; Elastic energy; Earthquakes

1. Introduction

Previously we have studied the effects of superposition of the lunar and solar tides with respect to the elastic energy stored in the elastic mantle of the Earth [1–3]. The main focus was on the problem of the possible correlation of the variations in this elastic energy with earthquake events [4–7]. In our last paper [7], first we studied the variations in the elastic energy caused by the mutual combination of rotational and lunisolar tides. The dates of phenomenal earthquakes at Hokkaido (25 September 2003) and Sumatra (26 December 2004) with magnitudes 8.5 and 9.0 respectively have been predicted with a high accuracy to within about 20 h [1, 7]. In the above-mentioned paper we developed our approach to the analysis of the tension state of the Earth perturbed by the combination of the rotational and lunisolar tides in the elastic mantle of the Earth. We have studied the behaviour of the graph of the variations in the elastic energy on

*Corresponding author. Email: yuri.barkin@ua.es

Astronomical and Astrophysical Transactions
ISSN 1055-6796 print/ISSN 1476-3540 online © 2007 Taylor & Francis
http://www.tandf.co.uk/journals
DOI: 10.1080/10556790601017224

different timescales (the last century, the last few decades, the period 1000–2100 and others) with different degrees of detail. As a result of the preliminary studies we have shown that the dates of the extreme variations in the elastic energy of the Earth correlate with the dates of large quakes (on the basis of data in the period 1997–2004). An important regularity has been discovered for very large earthquakes with a magnitude of not less than 8.0 in the last 105 years (25 events). For the majority of these events their dates are situated close to the dates of the extreme values of the average curve of the discussed elastic energy (for the 'roots of the trees').

2. Treatment of the problem; the tidal perturbing potential from a system of celestial bodies

The Earth's mantle is a non-spherical inhomogeneous cover with a quasiconcentric distribution of densities. Let R_0 be the mean radius of the Earth, and $\tilde{R}_0$ the radius of the larger sphere which we can place in the mantle's cavity (we assume that the centre of this sphere coincides with the Earth's centre of mass).

We shall consider the mantle as a deformable elastic body which is subjected to the attraction of a system of external celestial bodies P_σ ($\sigma = 1, 2, \ldots, N$) (in particular from the Moon and the Sun). The deformations of the Earth produced by these bodies will be described by the classical model [8], which was studied in detail in [9–11] in order to construct the rotation theory of the deformable Earth.

Let us consider the main Cartesian reference system Cxyz with the origin at the Earth's centre of mass and with axes directed along its principal axes of inertia in the undeformed state. Let $\boldsymbol{r}$ and $\boldsymbol{r}'$ be the radius vectors of an arbitrary point (or an elementary volume dm) of the mantle in the absence of deformations and in the deformable state. As usual, we assume that the particles of the deformable solid mantle deviate slightly from the positions that they occupy in the absence of deformation. The small displacement vector $\boldsymbol{u}(\boldsymbol{r}, t)$ in the considered case is presented as a sum of the elastic displacements of the mantle's particles caused by every external celestial body separately:

$$\boldsymbol{r}(t) = \boldsymbol{r}_0 + \boldsymbol{u}(\boldsymbol{r}_0, t) \Longrightarrow (x, y, z)(t) = (x_0, y_0, z_0) + (u, v, w)(x_0, y_0, z_0; t), \tag{1}$$

$$\boldsymbol{u} = \boldsymbol{u}_\omega + \sum_{\sigma=1}^{N} \boldsymbol{u}_\sigma, \quad u = u_\omega + \sum_{\sigma=1}^{N} u_\sigma, \quad v = v_\omega + \sum_{\sigma=1}^{N} v_\sigma, \quad w = w_\omega + \sum_{\sigma=1}^{N} w_\sigma, \tag{2}$$

where (x, y, z) are the positional coordinates of the particle of the deformable body, and (x_0, y_0, z_0) are the positional coordinates that the same particle would have in the absence of deformations, (u, v, w) being the components of the full displacement vector caused by the system of external bodies, and $(u_\sigma, v_\sigma, w_\sigma)$ being the components of the displacement vector caused by the concrete body P_σ.

2.1 *Deformations caused by the gravitational attraction of external celestial bodies*

The components of the displacement vector $\boldsymbol{u}_0$ during the deformation of mantle under Newtonian attraction of the external bodies (the Moon and the Sun) are defined as [8]

$$(u_\sigma, v_\sigma, w_\sigma) = \sum_{n=1}^{\infty} F_n(r_0) \frac{\partial W_{\sigma n}}{\partial (x, y, z)} + G_n(r_0)(x, y, z) W_{\sigma n}, \tag{3}$$

where $W_{\sigma n}$ is a harmonic of the nth order of the tidal potential caused by the gravitational attraction of the perturbing body P_σ, and where $F_n(r)$ and $G_n(r)$ are Takeuchi functions depending only on the variable r.

We shall study the deformation produced in the Earth's mantle due to its rotation, taking into account the permanent axial rotation with unperturbed angular velocity Ω and the perturbations in the axial rotation and in the pole motion of the Earth. We shall use spherical coordinates whose origin are at the centre of the body to determine the point $\mathrm{P}(r, \alpha, \beta)$ at which we evaluate the potential, and we shall determine the orientation of the angular velocity $\boldsymbol{\omega}$ from the spherical coordinates $\boldsymbol{\omega} = (\omega, \alpha_\omega, \beta_\omega)$.

2.2 *Rotational potential*

Because of its own rotation an elastic body is subjected to deformations. The disturbing rotational potential determining deformations per unit mass is determined by the well-known formula [9]

$$W_\omega = \frac{1}{3}\omega^2 r^2 - \frac{1}{3}\omega^2 r^2 P_2(\cos\gamma), \quad \cos\gamma = \frac{\boldsymbol{r}\cdot\boldsymbol{\omega}}{r\omega}, \tag{4}$$

where $\boldsymbol{\omega}$ is the angular velocity of the body, $\boldsymbol{r}$ is the radius vector of a body point and ω is the modulus of the angular velocity; $r = |\boldsymbol{r}| \cdot \gamma$ is the angle between the direction of the angular velocity and the radius vector $\boldsymbol{r}$.

Previously it was shown that, considering a symmetrically spherical Earth, under the influence of the perturbing rotational potential (4) the inertial tensor suffers an increase J_ω given by

$$J_\omega = D_\omega \begin{pmatrix} R_0 - R_2\cos(2\alpha_\omega) & -R_2\sin(2\alpha_\omega) & -R_1\cos\alpha_\omega \\ -R_2\sin(2\alpha_\omega) & R_0 + R_2\cos(2\alpha_\omega) & -R_1\sin\alpha_\omega \\ -R_1\cos\alpha_\omega & -R_1\sin\alpha_\omega & -2R_0 \end{pmatrix}, \tag{5}$$

where

$$R_0 = \frac{1}{2}(3\cos^2\beta_\omega - 1), \quad R_1 = 3\sin\beta_\omega\cos\beta_\omega, \quad R_2 = \frac{3}{2}\sin^2\beta_\omega, \tag{6}$$

α_ω and β_ω being the longitude and colatitude respectively of the vector $\boldsymbol{\omega}$, and where the coefficient D_ω is determined from its dependence on the elastic properties of the body by the integral I_r:

$$D_\omega = -\frac{4\pi}{15}\frac{\omega^2}{3}I_r, \quad I_r = \int_r \left(2\rho_0 r^4[5F_2(r) + r^2G_2(r)] - r^5\frac{\mathrm{d}\rho_0}{\mathrm{d}r}[2F_2(r) + r^2G_2(r)]\right)\mathrm{d}r. \tag{7}$$

In the integrand (7), $F_2(r)$ and $G_2(r)$ are functions determined from the theory of elasticity [9, 10]. ρ_0 is the density of the concentric mass distribution.

In the general case, D_r is a function of time determined from the temporal dependence of the modulus of the angular velocity ω. In this connection we introduce also the unperturbed value of this coefficient:

$$D_{\omega_0} = -\frac{4\pi}{15}\frac{\omega_0^2}{3}I_r. \tag{8}$$

Here $\omega = \omega_0$ is an unperturbed value of angular velocity. Thus we have the simple relation

$$D_\omega = D_{\omega_0}\frac{\omega_0^2}{\omega^2}. \tag{9}$$

The evaluation of the elastic parameter D_{ω_0} was given in [9, 10]: $D_{\omega_0} = -2.845\,379 \times 10^{41}$ c.g.s.

2.3 *The displacement vector of rotational deformations*

The rotational tidal potential (4)–(7) can be presented in the following generalized form [10]:

$$W_2^{(\omega)} = \frac{1}{3}\omega^2 r^2 - \frac{1}{3}\omega^2 r^2 (3\sin^2\beta) P_2(\cos\gamma), \quad W_\omega = \sum_{m=0}^{2} W_{\omega 2m}, \tag{10}$$

where $W_{\sigma n}$ is a harmonic of the nth order of the tidal potential caused by gravitational attraction of the perturbing body P_σ:

$$W_{\sigma n} = \frac{Gm_\sigma}{r_\sigma} \sum_{n=2}^{\infty} \left(\frac{r}{r_\sigma}\right)^n P_n(\cos S_\sigma), \tag{11}$$

where G is the gravitational constant, P_n are Legendre functions and S_σ is the angle between the radius vector of the perturbing body with coordinates x_σ, y_σ, z_σ and an arbitrary point (x, y, z) of the elastic mantle.

Now we introduce the spherical coordinates r, θ, φ for the elementary mass dm of the mantle and the spherical coordinates ω, δ_ω, α_ω for the angular velocity vector (here θ and δ_ω are the latitude and colatitude respectively; φ and α_ω are the longitudes). With the Cartesian coordinates (x, y, z) of the mantle point and the components of the angular velocity $\boldsymbol{\omega} = (p, q, r)$, these variables are connected by the formulae

$$\begin{aligned} x &= r\cos\varphi\cos\lambda, \quad y = r\cos\varphi\sin\lambda, \quad z = r\sin\varphi; \\ p &= \omega\sin\delta_\omega\cos\alpha_\omega, \quad q = \omega\sin\delta_\omega\sin\alpha_\omega, \quad r = \omega\cos\delta_\omega; \\ \cos\gamma &= \cos\varphi\sin\delta_\omega\cos(\lambda - \alpha_\omega) + \sin\varphi\cos\delta_\omega. \end{aligned} \tag{12}$$

All coordinates (5) are defined with respect to the main reference system Cxyz.

Let us now use the formula for the multiplication of Legendre functions:

$$P_n(\cos S_\sigma) = \sum_{m=0}^{2} q_{nm} P_2^m(\sin\delta_\omega) P_{nm}^m(\cos\theta)[\cos(m\alpha_\omega)\cos(m\varphi) + \sin(m\alpha_\omega)\sin(m\varphi)], \tag{13}$$

where

$$q_{2m} = \frac{(2-m)!}{(2+m)!}(2 - \delta_{0m}) = \frac{2(2-m)!}{(2+m)!\delta_m} \tag{14}$$

are numerical coefficients (here δ_{0m} is the Kronecker symbol and $\delta_m = \delta_{0m} + 1$).

Now we can present the general tidal potential in the special form that was used for calculations of the tidal energy in the case of one perturbing body [10]. Here we shall follow the general features of the method used in [10]. So we have the following:

$$\begin{aligned} W_2^{(\omega)} &= \sum_{m=0}^{2} W_{2m}^{(\omega)}, \\ W_{2m}^{(\omega)} &= r^2(A_{\mathrm{c}2m}^{\omega} B_{\mathrm{c}2m} + A_{\mathrm{s}2m}^{\omega} B_{\mathrm{s}2m}), \end{aligned} \tag{15}$$

where

$$\begin{aligned} A^{\omega}_{cnm} &= -\frac{\omega^2}{3} q_{2m} P_2^m(\sin\delta_\omega)\cos(m\alpha_\omega), \\ A^{\omega}_{snm} &= -\frac{\omega^2}{3} q_{2m} P_2^m(\sin\delta_\omega)\sin(m\alpha_\omega), \\ B_{cnm} &= P_n^m(\cos\theta)\cos(m\varphi), \\ B_{snm} &= P_n^m(\cos\theta)\sin(m\varphi). \end{aligned} \tag{16}$$

Thus, with $q_{20} = 1$, $q_{21} = 1/3$ and $q_{22} = 1/12$, we obtain the expression

$$\begin{aligned} W_2^{(\omega)} = \frac{1}{3}\omega^2 r^2 - \frac{1}{3}\omega^2 r^2 \Big\{ & P_2(\sin\delta_\omega) P_2(\cos\theta) \\ & + \frac{1}{3} P_2^{(1)}(\sin\delta_\omega) P_2^{(1)}(\cos\theta)(\cos\alpha_\omega\cos\varphi + \sin\alpha_\omega\sin\varphi) \\ & + \frac{1}{12} P_2^{(2)}(\sin\delta_\omega) P_2^{(2)}(\cos\theta)[\cos(2\alpha_\omega)\cos(2\varphi) + \sin(2\alpha_\omega)\sin(2\varphi)] \Big\}. \end{aligned} \tag{17}$$

We study the tidal deformations of a celestial body which moves and rotates in the gravitational field of the other celestial bodies P_σ ($\sigma = 1, 2, \ldots, N$) of the system. The general tidal potential from the system of these bodies can be represented in the following form [10]:

$$\begin{aligned} W^{(G)} &= \sum_{\sigma=1}^{N}\sum_{n=2}^{\infty} W^{(G)}_{\sigma n} = \sum_{\sigma=1}^{N}\sum_{n=2}^{\infty}\sum_{m=0}^{n} W^{(G)}_{\sigma nm}, \\ W^{(G)} &= \sum_{n=2}^{\infty}\sum_{m=0}^{n} W^{(G)}_{nm}, \quad W^{(G)}_{nm} = \sum_{\sigma=1}^{N} W^{(G)}_{\sigma nm}, \\ W_{2m} &= W^{(\omega)}_{2m} + \sum_{\sigma=1}^{N} W^{(G)}_{\sigma 2m} \quad (m = 0, 1, 2), \end{aligned} \tag{18}$$

where $W^{(G)}_{\sigma n}$ is a harmonic of the nth order of the tidal potential caused by the gravitational attraction of the perturbing body P_σ:

$$W^{(G)}_{\sigma n} = \frac{G m_\sigma}{r_\sigma} \sum_{n=2}^{\infty} \left(\frac{r}{r_\sigma}\right)^n P_n(\cos S_\sigma), \tag{19}$$

where G is the gravitational constant, P_n are Legendre functions and S_σ is the angle between the radius vector of the perturbing body with coordinate x_σ, y_σ, z_σ and an arbitrary point (x, y, z) of the elastic mantle.

Now we introduce the spherical coordinates r, θ, φ for the elementary mass dm of the mantle and the spherical coordinates r_σ, δ_σ, α_σ for the perturbing body P_σ (here θ and δ_σ are the latitude and colatitude respectively; φ and α_σ are the longitudes). With the Cartesian coordinates (x, y, z) of the mantle point and the Cartesian coordinates $(x_\sigma, y_\sigma, z_\sigma)$ of the perturbing body, these variables are connected by the formulae

$$\begin{aligned} x &= r\cos\varphi\cos\lambda, \quad y = r\cos\varphi\sin\lambda, \quad z = r\sin\varphi; \\ x_\sigma &= r_\sigma\sin\delta_\sigma\cos\alpha_\sigma, \quad y_\sigma = r_\sigma\sin\delta_\sigma\sin\alpha_\sigma, \quad z_\sigma = r_\sigma\cos\delta_\sigma. \end{aligned} \tag{20}$$

All the coordinates (20) are defined with respect to the main reference system Cxyz.

We now find that

$$P_n(\cos S_\sigma) = \sum_{m=0}^{n} \{q_{nm} P_n^m(\sin\delta_\sigma) P_n^m(\cos\theta)[\cos(m\alpha_\sigma)\cos(m\varphi) + \sin(m\alpha_\sigma)\sin(m\varphi)]\}, \tag{21}$$

where

$$q_{nm} = \frac{(n-m)!}{(n+m)!}(2-\delta_{0m}) = \frac{2(n-m)!}{(n+m)!\delta_m} \tag{22}$$

are numerical coefficients (here δ_{0m} is the Kronecker symbol and $\delta_m = \delta_{0m} + 1$).

Now we can present the general tidal potential in the special form that was used for calculations of the tidal energy in the case of one perturbing body [10]. Here we shall follow the general features of the method used in [10]. So we have the following:

$$W = W^{(G)} + W^{(\omega)} = W_1^{(\omega)} + W_2^{(\omega)} + \sum_{\sigma=1}^{N}\sum_{n=2}^{\infty} W_{\sigma n}^{(G)} = \sum_{n=2}^{\infty}\sum_{m=0}^{n} r^n (A^*_{cnm} B_{cnm} + A^*_{snm} B_{snm}), \tag{23}$$

where

$$\begin{aligned}
A^*_{cnm} &= G\sum_{\sigma=1}^{N} \frac{m_\sigma}{r_\sigma^{n+1}} P_n^m(\sin\delta_\sigma)\cos(m\alpha_\sigma), \\
&\qquad\qquad (n > 2), \\
A^*_{snm} &= G\sum_{\sigma=1}^{N} \frac{m_\sigma}{r_\sigma^{n+1}} P_n^m(\sin\delta_\sigma)\sin(m\alpha_\sigma), \\
A^*_{c2\,m} &= \sum_{\sigma=1}^{N}\left(G\frac{m_\sigma}{r_\sigma^{n+1}} P_2^m(\sin\delta_\sigma)\cos(m\alpha_\sigma)\right) - \frac{\omega^2}{3} P_2^m(\sin\delta_\omega)\cos(m\alpha_\omega), \\
&\qquad\qquad (n = 2, \quad m = 0, 1, 2), \\
A^*_{s2\,m} &= \sum_{\sigma=1}^{N}\left(G\frac{m_\sigma}{r_\sigma^{n+1}} P_2^m(\sin\delta_\sigma)\sin(m\alpha_\sigma)\right) - \frac{\omega^2}{3} P_2^m(\sin\delta_\omega)\sin(m\alpha_\omega), \\
A^*_{c1\,m} &= -\frac{\omega^2}{3} P_1^m(\sin\delta_\omega)\cos(m\alpha_\omega), \\
&\qquad\qquad (n = 1,\ m = 0, 1), \\
A^*_{s1m} &= -\frac{\omega^2}{3} P_1^m(\sin\delta_\omega)\sin(m\alpha_\omega), \\
B_{cnm} &= P_n^m(\cos\theta)\cos(m\varphi), \\
&\qquad\qquad (n > 2, m = 0, 1) \\
B_{snm} &= P_n^m(\cos\theta)\sin(m\varphi).
\end{aligned} \tag{24}$$

For the perturbing potential W_{nm} from equations (23) and (24) a solution of the problem of elastic deformations can be presented by the Hergolz formulae in Cartesian coordinates [10]:

$$\begin{aligned} u &= \sum_{n=2}^{\infty} u_n = \sum_{n=2}^{\infty}\sum_{m=0}^{n}\left(F_n(r)\frac{\partial W_{nm}}{\partial x} + G_n(r)x\,W_{nm}\right),\\ v &= \sum_{n=2}^{\infty} v_n = \sum_{n=2}^{\infty}\sum_{m=0}^{n}\left(F_n(r)\frac{\partial W_{nm}}{\partial y} + G_n(r)y\,W_{nm}\right),\\ w &= \sum_{n=2}^{\infty} w_n = \sum_{n=2}^{\infty}\sum_{m=0}^{n}\left(F_n(r)\frac{\partial W_{nm}}{\partial z} + G_n(r)z\,W_{nm}\right),\\ W_{nm} &= r^n(A^*_{\mathrm{c}nm}B_{\mathrm{c}nm} + A^*_{\mathrm{s}nm}B_{\mathrm{s}nm}). \end{aligned} \tag{25}$$

For the perturbing potential $W_{\omega 2\,m}$ from equations (23) and (24) a solution of the problem of elastic deformations caused by rotation of the body can be presented in a similar form:

$$\begin{aligned} u &= u_2 = \sum_{m=0}^{2}\left(F_2(r)\frac{\partial W_{\omega 2\,m}}{\partial x} + G_2(r)x\,W_{\omega 2\,m}\right),\\ v &= v_2 = \sum_{m=0}^{2}\left(F_2(r)\frac{\partial W_{\omega 2\,m}}{\partial y} + G_2(r)y\,W_{\omega 2\,m}\right),\\ w &= w_2 = \sum_{m=0}^{2}\left(F_2(r)\frac{\partial W_{\omega 2\,m}}{\partial z} + G_2(r)z\,W_{\omega 2\,m}\right),\\ W_{\omega 2\,m} &= r^2(A^{\omega}_{\mathrm{c}2\,m}B_{\mathrm{c}2\,m} + A^{\omega}_{\mathrm{s}2\,m}B_{\mathrm{s}2\,m}). \end{aligned} \tag{26}$$

The solution (26) presents a linear superposition of the solutions of classical problem for one perturbing body. It is important to note that the form of solution (23) and (24) is identical with the classical formulae that were used in [10] for the calculation of the analytical expression for the energy of tides. It allows us to use almost all intermediate non-trivial analytical transformations of [10] to calculate the elastic energy for the more general case of the superposition of tides considered in this paper.

Here the functions $F_n(r)$ and $G_n(r)$, similar to $K_n(r)$, are functions of only r, which can be obtained as the solution of a system of ordinary differential equations. For Takeuchi's models and for the modern models 1066A and 1066B of the Earth given by Gilbert and Dziewonski [12] in the cases $n = 2, 3$, these functions were determined in [9–11]. These functions do not depend on the action of perturbing bodies.

In spherical coordinates the components of the displacement vector are determined by following well-known formulae:

$$\begin{aligned} u_r &= \sum_{n'=1}^{\infty}\frac{1}{r}l_{n'}W_{n'},\\ u_\theta &= \frac{1}{r}\sum_{n'=1}^{\infty}F_{n'}\frac{\partial W_{n'}}{\partial\theta},\\ u_\varphi &= \frac{1}{r\sin\theta}\sum_{n'=1}^{\infty}F_{n'}\frac{\partial W_{n'}}{\partial\varphi}, \end{aligned} \tag{27}$$

where

$$l_{n'} = n' F_{n'} + r^2 G_{n'}.$$

3. The elastic energy

If an elastic isotropic body, obeying the Hooke law, is deformed by the gravitational attraction of external celestial bodies, an elastic deformation energy is produced. This energy per unit volume is expressed as

$$E = \frac{\lambda}{2}(e_{xx} + e_{yy} + e_{zz})^2 + \mu(e_{xx}^2 + e_{yy}^2 + e_{zz}^2 + 2(e_{xy}^2 + e_{xz}^2 + e_{yz}^2), \tag{28}$$

e_{ij} being components of the deformation, which relate to the displacement vector $\boldsymbol{u} = (u, v, w)$ by means of

$$\begin{aligned} e_{xx} &= \frac{\partial u}{\partial x}, \quad e_{xy} = \frac{1}{2}\left(\frac{\partial u}{\partial y} + \frac{\partial v}{\partial x}\right), \\ e_{yy} &= \frac{\partial v}{\partial y}, \quad e_{xz} = \frac{1}{2}\left(\frac{\partial u}{\partial z} + \frac{\partial w}{\partial x}\right), \\ e_{zz} &= \frac{\partial w}{\partial z}, \quad e_{yz} = \frac{1}{2}\left(\frac{\partial v}{\partial z} + \frac{\partial w}{\partial y}\right). \end{aligned} \tag{29}$$

The components of the displacement vector were obtained as a solution of the problem of the theory of elasticity. They are determined by equations (23), (24) and (26).

To obtain an expression for the deformation energy it is sufficient to insert the series (26) into equations (28) and (29) and then to calculate the corresponding volume integral spread over the entire elastic shell in its initial state:

$$E_{\mathrm{d}} = \int_r^R \int_0^\pi \int_0^{2\pi} E r^2 \sin\theta \, \mathrm{d}r \, \mathrm{d}\theta \, \mathrm{d}\varphi, \tag{30}$$

where R and r are the mean radius and the inferior radius respectively of the elastic shell.

Here we shall use detailed calculations of the integral (30) for the classical problem of the lunar tides [9, 10] but we shall take into account some generalization of our problem to the system of perturbing bodies.

In the above-mentioned papers, to calculate the energy (30), spherical coordinates have been used. In this case the spherical components of the displacement vector are defined by the following formulae [8]:

$$\begin{aligned} u_r &= \sum_{n=1}^{\infty} u_{rn} = \sum_{n=1}^{\infty} \sum_{m=0}^{n} \left(\frac{n}{r} F_n(r) + r G_n(r)\right) W_{nm}, \\ u_\theta &= \sum_{n=1}^{\infty} u_{\theta n} = \sum_{n=1}^{\infty} \sum_{m=0}^{n} \left(\frac{1}{r} F_n(r)\right) \frac{\partial W_{nm}}{\partial \theta}, \\ u_\varphi &= \sum_{n=1}^{\infty} u_{\varphi n} = \sum_{n=1}^{\infty} \sum_{m=0}^{n} \left(\frac{1}{r \sin\theta} F_n(r)\right) \frac{\partial W_{nm}}{\partial \varphi}. \end{aligned} \tag{31}$$

On the other hand, in these coordinates the elastic energy per unit volume is

$$E = \frac{\lambda}{2}(e_{rr} + e_{\theta\theta} + e_{\varphi\varphi})^2 + \mu(e_{rr}^2 + e_{\theta\theta}^2 + e_{\varphi\varphi}^2 + 2(e_{r\theta}^2 + e_{r\varphi}^2 + e_{\theta\varphi}^2), \tag{32}$$

where the components of the deformations are

$$\begin{aligned}
e_{rr} &= \frac{\partial u_r}{\partial r}, \quad e_{\theta\theta} = \frac{1}{r}\frac{\partial u_\theta}{\partial \theta} + \frac{u_r}{r}, \\
e_{\varphi\varphi} &= \frac{1}{r\sin\theta}\frac{\partial u_\varphi}{\partial \varphi} + \frac{1}{r}(u_r + u_\theta \cot\theta), \\
e_{r\theta} &= \frac{1}{2}\left(\frac{1}{r}\frac{\partial u_r}{\partial \theta} - \frac{u_r}{r} + \frac{\partial u_\theta}{\partial r}\right), \\
e_{r\varphi} &= \frac{1}{2}\left(\frac{1}{r\sin\theta}\frac{\partial u_r}{\partial \varphi} - \frac{u_\varphi}{r} + \frac{\partial u_\varphi}{\partial r}\right), \\
e_{\theta\varphi} &= \frac{1}{2}\left(\frac{1}{r\sin\theta}\frac{\partial u_\theta}{\partial \varphi} - \frac{1}{r}\cot\theta u_\varphi + \frac{1}{r}\frac{\partial u_\varphi}{\partial \theta}\right).
\end{aligned} \tag{33}$$

Inserting equations (33) into equation (32), and taking into account the fact that the spherical harmonics W_n verify the ratio,

$$\frac{\partial W_n}{\partial r} = \frac{n}{r}W_n, \tag{34}$$

After some calculations we obtain [10]

$$e_{ST} = \sum_{n,m} e_{STnm}, \quad (S, T = r, \theta, \varphi), \sum_{n,m} = \sum_{n=1}^{\infty}\sum_{m=0}^{n}, \tag{35}$$

and the coefficients in equation (35) are defined by the following formulae:

$$\begin{aligned}
e_{rrnm} &= Q_{1n}W_{nm}, \quad e_{\theta\theta nm} = Q_{3n}\frac{\partial^2 W_{nm}}{\partial\theta^2} + Q_{2n}W_{nm}, \\
e_{\varphi\varphi nm} &= Q_{3n}\frac{1}{\sin^2\theta}\frac{\partial^2 W_{nm}}{\partial\varphi^2} + Q_{2n}W_{nm} + Q_{3n}\cot\theta\frac{\partial W_{nm}}{\partial\theta}, \\
e_{r\theta nm} &= \frac{1}{2}Q_{4n}\frac{\partial W_{nm}}{\partial\theta}, \quad e_{r\varphi nm} = \frac{1}{2\sin\theta}Q_{4n}\frac{\partial W_{nm}}{\partial\varphi}, \\
e_{\theta\varphi nm} &= Q_{3n}\left(\frac{1}{\sin\theta}\frac{\partial^2 W_{nm}}{\partial\theta\,\partial\varphi} - \cot\theta\frac{\partial W_{nm}}{\partial\varphi}\right).
\end{aligned} \tag{36}$$

In equation (36) the following new notation was used:

$$\begin{aligned}
Q_{1n} &= n\frac{\dot{F}_n}{r} + n(n-1)\frac{F_n}{r^2} + \dot{G}_n r + (n+1)G_n, \quad Q_{2n} = n\frac{F_n}{r^2} + G_n, \\
Q_{3n} &= \frac{F_n}{r^2}, \quad Q_{4n} = \frac{\dot{F}_n}{r} + 2(n-1)\frac{F_n}{r^2} + G_n, \quad \dot{F}_n = \frac{\mathrm{d}F_n}{\mathrm{d}r}.
\end{aligned} \tag{37}$$

In this notation the deformation energy can be presented in the following way:

$$E = \sum_{n,m}\sum_{n',m'} E_{nn'mm'}, \tag{38}$$

where

$$E_{nn'mm'} = \frac{\lambda}{2}(e_{rrnm} + e_{\theta\theta nm} + e_{\varphi\varphi nm})(e_{rrn'm'} + e_{\theta\theta n'm'} + e_{\varphi\varphi n'm'}) + \mu[e_{rrnm}e_{rrn'm'} + e_{\theta\theta nm}e_{\theta\theta n'm'} + e_{\varphi\varphi nm}e_{\varphi\varphi n'm'} + 2(e_{r\theta nm}e_{r\theta n'm'} + e_{r\varphi nm}e_{r\varphi n'm'} + e_{\theta\varphi nm}e_{\theta\varphi n'm'})]. \tag{39}$$

After some reduction of equations (38) and (21) the calculations of the energy integral (30) are reduced to calculations of the series table integrals and some integrals of the standard combinations of the Legendre associated functions and their derivatives. Also we should point out that all integrations with respect to the angular variables θ and φ are identical with those in [10, 11].

From the above remarks and using the full series of calculations in [10, 11], we obtain the final expression for the deformation energy (30) in the following compact form:

$$E_{\mathrm{d}} = \sum_{n=2}^{\infty}\sum_{m=0}^{n}\frac{2\pi}{2n+1}q_{nm}\left(I_n^{\lambda} + 2I_n^{\mu}\right)\left[(A^*_{cnm})^2 + (A^*_{snm})^2\right], \tag{40}$$

where

$$q_{nm} = \frac{(n-m)!}{(n+m)!}(2-\delta_{0m}),$$

and the elastic constants I_n^{λ} and I_n^{μ} are defined by the following integrals:

$$I_n^{\lambda} = \int_r^R \lambda r^{2(n+1)}\left(n\frac{\dot{F}_n}{r} + +r\dot{G}_n + (n+3)G_n\right)^2 \mathrm{d}r, \tag{41}$$

$$I_n^{\mu} = \int_r^R \mu r^{2(n+1)}\left[n(4n^3 - 4n^2 - n + 1)\frac{F_n^2}{r^4} + 2n(2n^2 - n - 1)F_n\left(\frac{\dot{F}_n}{r^3} + \frac{G_n}{r^2}\right) + 2n(n-1)\frac{F_n\dot{G}_n}{r} + \frac{1}{2}n(3n+1)\frac{\dot{F}_n^2}{r^2} + 3n(n+1)\frac{\dot{F}_nG_n}{r} + 2n\dot{G}_n\dot{F}_n + \frac{1}{2}(3n^2 + 5n + 6)G_n^2 + 2(n+1)G_n\dot{G}_nr + \dot{G}_n^2r^2\right]\mathrm{d}r. \tag{42}$$

Using equations (26) and (40)–(42) now, we obtain a new formula for the energy:

$$E_{\mathrm{d}} = \sum_{n=2}^{\infty}\frac{2\pi}{2n+1}\left(I_n^{\lambda} + 2I_n^{\mu}\right)\sum_{m=0}^{n}q_{nm}\left[(A^*_{cnm})^2 + (A^*_{snm})^2\right]$$

$$
\begin{aligned}
&= \frac{2}{5}\pi \left(I_2^{\lambda} + 2I_2^{\mu}\right) \Bigg[\sum_{m=0}^{2} q_{2m} \left(-\frac{\omega^2}{3} P_2^m(\sin\delta_\omega)\cos(m\alpha_\omega) \right. \\
&\quad \left. + G \sum_{\sigma=1}^{N} \frac{m_\sigma}{r_\sigma^3} P_2^m(\sin\delta_\sigma)\cos(m\alpha_\sigma) \right)^2 \\
&\quad + \sum_{m=0}^{2} q_{2m} \left(-\frac{\omega^2}{3} P_2^m(\sin\delta_\omega)\sin(m\alpha_\omega) + \sum_{\sigma=1}^{N} \frac{m_\sigma}{r_\sigma^3} P_2^m(\sin\delta_\sigma)\sin(m\alpha_\sigma) \right)^2 \Bigg] \\
&\quad + \sum_{n=3}^{\infty} \frac{2\pi G^2}{2n+1} \left(I_n^{\lambda} + 2I_n^{\mu}\right) \sum_{m=0}^{n} q_{nm} \Bigg[\left(\sum_{\sigma=1}^{N} \frac{m_\sigma}{r_\sigma^{n+1}} P_n^m(\sin\delta_\sigma)\cos(m\alpha_\sigma) \right)^2 \\
&\quad + \left(\sum_{\sigma=1}^{N} \frac{m_\sigma}{r_\sigma^{n+1}} P_n^m(\sin\delta_\sigma)\sin(m\alpha_\sigma) \right)^2 \Bigg] \\
&= \frac{2\pi}{5} \left(I_2^{\lambda} + 2I_2^{\mu}\right) \sum_{\sigma=1}^{N} G^2 \left(\frac{m_\sigma}{r_\sigma^3} \right)^2 \sum_{m=0}^{n} q_{2m} \left\{ \left[P_2^m(\sin\delta_\sigma)\cos(m\alpha_\sigma) \right]^2 \right. \\
&\quad \left. + \left[P_2^m(\sin\delta_\sigma)\sin(m\alpha_\sigma) \right]^2 \right\} \\
&\quad + \frac{2\pi}{45} \left(I_2^{\lambda} + 2I_2^{\mu}\right) \omega^4 \sum_{m=0}^{n} q_{2m} \left\{ \left[P_2^m(\sin\delta_\omega)\cos(m\alpha_\omega) \right]^2 + \left[P_2^m(\sin\delta_\omega)\sin(m\alpha_\omega) \right]^2 \right\} \\
&\quad - \frac{4\pi}{15} \left(I_2^{\lambda} + 2I_2^{\mu}\right) \omega^2 G^2 \sum_{\sigma=1}^{N} \frac{m_\sigma}{r_\sigma^3} \sum_{m=0}^{n} q_{2m} \left\{ P_2^m(\sin\delta_\omega) \right. \\
&\quad \left. \times P_2^m(\sin\delta_\sigma) \left[\cos(m\alpha_\omega)\cos(m\alpha_\sigma) + \sin(m\alpha_\omega)\sin(m\alpha_\sigma) \right] \right\} \\
&\quad + \frac{4\pi}{5} \left(I_2^{\lambda} + 2I_2^{\mu}\right) G^2 \sum_{\substack{i,j=1 \\ i>j}}^{N} \frac{m_i}{r_i^3} \frac{m_j}{r_j^3} \sum_{m=0}^{n} q_{2m} \left\{ P_2^m(\sin\delta_i) \right. \\
&\quad \left. \times P_2^m(\sin\delta_j) \left[\cos(m\alpha_i)\cos(m\alpha_j) + \sin(m\alpha_i)\sin(m\alpha_j) \right] \right\} \\
&\quad + \sum_{n=3}^{\infty} \frac{2\pi}{2n+1} \left(I_n^{\lambda} + 2I_n^{\mu}\right) G^2 \sum_{\sigma=1}^{N} \left(\frac{m_\sigma}{r_\sigma^{n+1}} \right)^2 \sum_{m=0}^{n} q_{nm} \left\{ \left[P_n^m(\sin\delta_\sigma)\cos m\alpha_\sigma \right]^2 \right. \\
&\quad \left. + \left[P_n^m(\sin\delta_\sigma)\sin m\alpha_\sigma \right]^2 \right\} \\
&\quad + 2 \sum_{n=2}^{\infty} \frac{2\pi G^2}{2n+1} \left(I_n^{\lambda} + 2I_n^{\mu}\right) \sum_{\substack{i,j=1 \\ i>j}}^{N} \frac{m_i}{r_i^{n+1}} \frac{m_j}{r_j^{n+1}} \sum_{m=0}^{n} q_{nm} \left\{ P_n^m(\sin\delta_i) \right. \\
&\quad \left. \times P_n^m(\sin\delta_j) \left[\cos(m\alpha_i)\cos(m\alpha_j) + \sin(m\alpha_i)\sin(m\alpha_j) \right] \right\}. \qquad (43)
\end{aligned}
$$

The additional spherical theorem lets us introduce the very simple relations

$$
\sum_{m=0}^{n} q_{nm} \left\{ \left[P_n^m(\sin\delta_\sigma)\cos(m\alpha_\sigma) \right]^2 + \left[P_n^m(\sin\delta_\sigma)\sin(m\alpha_\sigma) \right]^2 \right\}
$$

$$
\begin{aligned}
&= \sum_{m=0}^{n} q_{nm} \left\{ P_n^m(\sin\delta_\sigma) P_n^m(\sin\delta_\sigma) \left[\cos(m\alpha_\sigma)\cos(m\alpha_\sigma)\right.\right. \\
&\quad \left.\left. + \sin(m\alpha_\sigma)\sin(m\alpha_\sigma)\right]\right\} = P_n(\cos 0) = 1, \\
&\sum_{m=0}^{n} q_{nm} \left\{ P_n^m(\sin\delta_i) P_n^m(\sin\delta_j) \left[\cos(m\alpha_i)\cos(m\alpha_j)\right.\right. \\
&\quad \left.\left. + \sin(m\alpha_i)\sin(m\alpha_j)\right]\right\} = P_n(\cos S_{ij}). \qquad (44) \\
&\sum_{m=0}^{n} q_{nm} \left\{ P_n^m(\sin\delta_\omega) P_n^m(\sin\delta_\sigma) \left[\cos(m\alpha_\omega)\cos(m\alpha_\sigma) + \sin(m\alpha_\omega)\sin(m\alpha_\sigma)\right]\right\} \\
&\quad = P_n(\cos\gamma_\sigma).
\end{aligned}
$$

Here S_{ij} is the angle between the radius vectors of the bodies P_i and P_j with longitudes and latitudes (α_i, δ_i) and (α_j, δ_j) respectively. Here γ_σ is the angle between radius vector of the body P_σ and the angular velocity vector $\boldsymbol{\omega}$ with longitudes and latitudes $(\alpha_\sigma, \delta_\sigma)$ and $(\alpha_\omega, \delta_\omega)$ respectively.

As a result, we present the full expression for the elastic energy of the planet caused by rotational and gravitational tides and their mutual coupling in the following form:

$$
\begin{aligned}
E_{\mathrm{d}} = e_2 &\left(\frac{\omega^4}{9} + G^2 \sum_{i=1}^{N} \frac{m_i^2}{r_i^6} + \frac{2}{3}\omega^2 G \sum_{\sigma=1}^{N} \frac{m_i}{r_\sigma^3} P_2(\gamma_\sigma) + 2G^2 \sum_{\substack{i,j=1 \\ i>j}}^{N} \frac{m_i m_j}{r_i^3 r_j^3} P_2(S_{ij}) \right) \\
&+ \sum_{i=1}^{N} \sum_{n=3}^{\infty} e_n \left(\frac{m_i}{r_i^{n+1}} \right)^2 + 2 \sum_{\substack{i,j=1 \\ i>j}}^{N} \sum_{n=3}^{\infty} e_n \frac{m_i}{r_i^{n+1}} \frac{m_j}{r_j^{n+1}} P_n(S_{ij}), \qquad (45)
\end{aligned}
$$

where we have introduced the new elastic parameters

$$
e_n = \frac{2\pi G^2}{2n+1} \left(I_n^\lambda + 2 I_n^\mu \right). \qquad (46)
$$

Thus equations (28) and (29) determine the elastic energy E_d as a function of the internal structure of the external shell (through I_n^λ and I_n^μ) and of the mass m_σ and the distance r_σ of the perturbing body but not depending, however, on its angular position.

In equation (45) we have especially allocated (in the first line) the main terms of the elastic energy which combine the following: firstly,

$$
E_{\mathrm{R}} = e_2 \frac{\omega^4}{9}
$$

is the elastic energy caused by the rotation of the planet; secondly,

$$
E_{\mathrm{T}} = \sum_{i=1}^{N} E_{\mathrm{T}i} = G^2 e_2 \sum_{i=1}^{N} \frac{m_i^2}{r_i^6}
$$

is the sum $E_{\mathrm{T}i} = m_i^2/r_i^6$ of the elastic energies of the planet caused by the tides produced by the separate perturbing celestial bodies P_i; thirdly,

$$E_{\mathrm{PP}} = 2G^2 e_2 \sum_{\substack{i,j=1 \\ i>j}}^{N} \frac{m_i m_j}{r_i^3 r_j^3} P_2(S_{ij})$$

is the elastic energy caused by the mutual combination of the tides produced by all the pairs of the perturbing bodies P_i and P_j; fourthly,

$$E_{\mathrm{RP}} = \frac{2}{3}\omega^2 G e_2 \sum_{\sigma=1}^{N} \frac{m_i}{r_\sigma^3} P_2(\gamma_\sigma)$$

is the elastic energy caused by the combination of the rotational tide and gravitational tides from all planets.

Here

$$e_2 = \frac{2\pi G^2}{5}\left(I_2^\lambda + 2I_2^\mu\right) \tag{47}$$

is the main elastic parameter of the second order.

In equation (47) we have

$$\begin{aligned} I_2^\lambda &= \int_r^R \lambda r^6 \left(2\frac{\dot{F}_2}{r} + r\dot{G}_2 + 5G_2\right)^2 \mathrm{d}r, \\ I_2^\mu &= \int_r^R \mu r^6 \left[30\frac{F_2^2}{r^4} + 20F_2\left(\frac{\dot{F}_2}{r^3} + \frac{G_2}{r^2}\right) + 4\frac{F_2\dot{G}_2}{r}\right. \\ &\quad \left. + 7\frac{\dot{F}_2^2}{r^2} + 18\frac{\dot{F}_2 G_2}{r} + 4\dot{G}_2\dot{F}_2 + 14G_2^2 + 6G_2\dot{G}_2 r + \dot{G}_2^2 r^2\right] \mathrm{d}r. \end{aligned} \tag{48}$$

4. The main components of the elastic energy of the Earth and their geodynamic role

In this section we provide an analysis of the different components of the elastic energy of the Earth caused by the rotational tide, by lunisolar tides and by their mutual contributions.

4.1 *The elastic energy of superposition of the Earth's tides from the Moon and the Sun*

We have obtained the formula for the elastic energy of the superposition of lunisolar tides. It was shown that the full energy is not the additive sum of the elastic energies of the separate tides and contains additional terms of mutual character, which play a significant role in the geodynamic life of the Earth. Correlation of the extreme variations in the elastic tidal energy of the Earth with earthquakes and moonquakes (in the period 1971–1976) was established. This regularity of the seismic process has been used to predict the dates of some large earthquakes in 2003. In particular the date of the phenomenal Hokkaido quake of 25 September 2003 ($M = 8.3$) was predicted with high accuracy [2, 4].

The oceanic and elastic shells of the Earth are deformed owing to lunar–solar attraction, which is due to the non-inertial rotational effects on pole motion and others. Different types of tide are observed on the Earth. We have considered also a new class of tides due to the inner nature of the Earth. They are caused by gravitational attraction of the moving core (rigid

and liquid). In a classical approximation all these tides are described by the linear theory of elasticity, and the full effect of the Earth's deformations is presented as a linear superposition of all the above-mentioned tides. The tensional state of the Earth is characterized by the elastic energy stored in the superposition of tides.

We have obtained the formula for the elastic energy of superposition of the tides. The full energy is not the additive sum of the elastic energies of separate tides; it also contains additional terms of mutual character. For example the mutual action of the Moon and the Sun on the Earth's mantle generates an additional energy with a maximum value of about 91.6% of the elastic energy E_M which is generated by the Moon. The full elastic energy of the lunisolar tides is changed in diapason: $212.6\%E_M$–$75.2\%E_M$. This large change is observed in every orbital period of the Moon.

These additional terms of energy are very important. They are sufficiently large and lead to notable, conditionally periodic variations in theelastic energy. So the above-mentioned variation of $137.4\%E_M$ is sufficiently higher than the variation in the energy caused by the eccentricity of the Moon's orbit, $67.8\%E_M$. The full variation in the elastic energy reaches $209.4\%E_M$. Also superposition of the rotational tide and the lunisolar tides leads to additional elastic energy terms.

Some of the elastic energy dissipates and is converted into warm energy and to an energization of different geodynamic processes in definite rhythms. In this paper we discuss the correlation of the extreme variations in the elastic tidal energy of the Earth with earthquakes and moonquakes (in the period 1971–1976). The established regularities of the seismic process have allowed us to predict the dates of some large earthquakes including the phenomenal Hokkaido quake of 25 September 2003 of magnitude $M = 8.3$.

We discuss here the expression for and the numerical value of the full energy of mantle deformations caused by lunar and solar attractions. Let us introduce the following geometrical and dynamic notation.

(i) x_M, y_M, z_M and x_S, y_S, z_S are the Cartesian coordinates of the Moon and the Sun, respectively.
(ii) $r_M = (x_M^2 + y_M^2 + z_M^2)^{1/2}$ and $r_S = (x_S^2 + y_S^2 + z_S^2)^{1/2}$ are the corresponding distances between the centre of mass of the Earth and the centres of masses of the Moon and the Sun, respectively.
(iii) $\cos S_{MS} = (x_M x_S + y_M y_S + z_M z_S)/r_M r_S$ is a cosine of the angle S_{MS} between the geocentric directions to the Sun and to the Moon.
(iv) a_M and a_S are unperturbed values of the major semiaxes of the lunar and solar orbits, respectively.
(v) e_M and e_S are unperturbed values of the eccentricities of the lunar and solar orbits, respectively.
(vi) e_2 is a elastic coefficient, which can be calculated, for example, on the basis of the classical solution of the elasticity theory problem of the lunisolar tide deformations for some models of the Earth [9].

In [9, 10] it was shown that the elastic energies stored in the Earth's tides caused by solar attraction are determined by the formulae

$$E_M = e_2 \frac{m_M^2}{r_M^6}, \quad E_S = e_2 \frac{m_S^2}{r_S^6}. \tag{49}$$

Previously we have shown that the full elastic energy E of lunisolar tides does not equal the sum of the above-mentioned energies [3]. This effect is caused by the quadratic structure of the elastic energy and by the geometry of the deformations of the Earth's mantle. Calculations

to prove this statement are not trivial and are not provided in this paper but we do give here the final expression for the elastic tidal energy of the Earth taking into account only the second harmonic:

$$E = e_2 \left(\frac{m_M^2}{r_M^6} + \frac{m_S^2}{r_S^6} + 2\frac{m_M m_S}{r_M^3 r_S^3} P_2(\cos S_{MS}) \right). \tag{50}$$

Equation (50) for the elastic energy contains the new additional term

$$E_{MS} = e_{MS} P_2(\cos S_{MS}), \tag{51}$$

where

$$e_{MS} = 2e_2 \frac{m_M m_S}{r_M^3 r_S^3}.$$

It is easy to see that $e_{MS} = E_{MS}$ when $S_{MS} = \pi/2, 3\pi/2$. In these cases the geocentric directions to the Moon and to the Sun are orthogonal. e_{MS} is the maximum value of the energy E_{MS}. Real values of E_{MS} change in the domain $(e_{MS}, -e_{MS}/2)$. It is worth remarking that the energy (50) presents only the main term (of second order) of the full expression for the elastic energy. A general equation was also obtained but we omit it in this paper. We confirm and shall show below that this additional term of energy is significant and plays an important role in geodynamic and geophysical processes.

Let us assume the following values for the parameters of the Earth–Moon–Sun system:

$$\begin{aligned} &1\,\text{AU} = 149\,597\,870\,\text{km}, \quad a_S = 1.000\,001\,017\,78\text{AU}, \quad a_M = 384\,000\,\text{km}, \\ &\frac{m_M}{m_E} = 0.012\,300\,038, \quad \frac{m_E}{m_S} = 3.003\,489\,6 \times 10^{-6}, \quad e_2 = 3.252 \times 10^{35}\,\text{c.g.s.} \end{aligned} \tag{52}$$

Also let us note some simple relations between the energies of the Sun and the Moon:

$$E_S = E_M \frac{m_S^2 r_M^6}{m_M^2 r_S^6}, \quad e_{MS} = 2(E_M E_S)^{1/2} = 2e_2 \frac{m_S m_M}{r_S^3 r_M^3}, \quad e_{MS} = 2E_M \frac{m_S r_M^3}{m_M r_S^3}. \tag{53}$$

Here e_{MS} is a coefficient mutiplied by $P_2(\cos S_{MS})$ in the additional term (51) in the full energy.

The unperturbed values of the energies are obtained from the basic values (52) and equations (53) with $r_M = a_M$ and $r_S = a_S$. Using 1 unit $= 10^{23}$ c.g.s. we determine the following:

$$\begin{aligned} E_M^{(0)} &= 5.473 \times 10^{23}\,\text{c.g.s.}, \quad E_S^{(0)} = 1.148 \times 10^{23}\,\text{c.g.s.}, \quad e_{MS}^{(0)} = 2(E_M^{(0)} E_S^{(0)})^{1/2} \\ &= 5.0132 \times 10^{23}\,\text{c.g.s.} \end{aligned} \tag{54}$$

The maximum value of the full lunisolar elastic energy of the Earth (the full Moon) is

$$E_{SM}^{\max} = E_S^{(0)} + E_M^{(0)} + 2(E_M^{(0)} E_S^{(0)})^{1/2} = 11.6342\,\text{c.g.s.} \tag{55}$$

The minimum value of this energy (the Moon in quarters) is

$$E_{SM}^{\min} = E_S^{(0)} + E_M^{(0)} - 2(E_M^{(0)} E_S^{(0)})^{1/2} = 4.1144 \times 10^{23}\,\text{c.g.s.} \tag{56}$$

The variations in the full energy are $\Delta E_{SM} = 3(E_M^{(0)} E_S^{(0)})^{1/2} = 7.5198 \times 10^{23}$ c.g.s. (every synodic month).

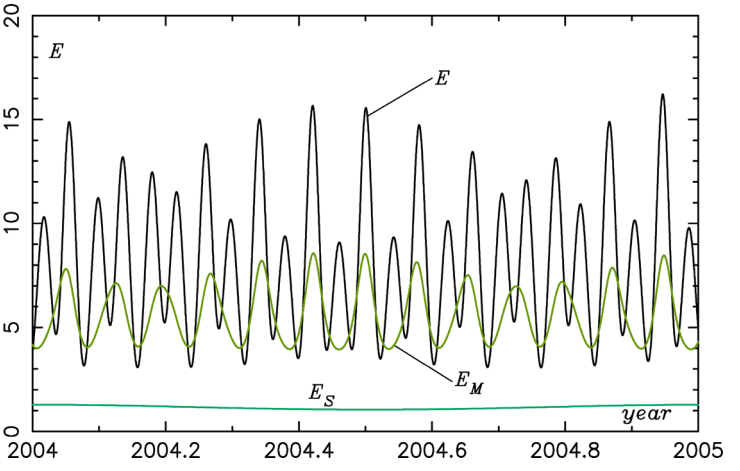

Figure 1. Variations in the elastic energy in 2004 (1unit = 10^{23} c.g.s.).

The lunar and solar eccentricity variations in the Earth's tidal energy (pericentre–apocentre positions) are determined by

$$\Delta E_{\mathrm{M}} = E_{\mathrm{M}}^{(0)}\left(\frac{1}{(1-e_{\mathrm{M}})^6} - \frac{1}{(1+e_{\mathrm{M}})^6}\right) = 0.6776E_{\mathrm{M}}^{(0)} = 3.7084 \times 10^{23}\,\text{c.g.s.}, \tag{57}$$

$$\Delta E_{\mathrm{S}} = E_{\mathrm{S}}^{(0)}\left(\frac{1}{(1-e_{\mathrm{S}})^6} - \frac{1}{(1+e_{\mathrm{S}})^6}\right) = 0.2015E_{\mathrm{S}}^{(0)} = 0.2314 \times 10^{23}\,\text{c.g.s.} \tag{58}$$

This means that the full variation in the tidal energy can be evaluated as 11.4596×10^{23} c.g.s.

Figure 1 illustrates the variations in the elastic energy of the Earth due to the influences of the Moon and the Sun and the variation in the full elastic energy of the Earth taking into account the mutual additional term (51). For illustration we have restricted the interval of time to 1 January 2004–1 January 2005. The behaviours of the curves in figure 1 are in accordance with simple evaluations of the average values and the amplitude of the variations in the elastic energy given above.

Now we consider and evaluate the other components of elastic energy caused by the Earth's rotation.

4.2 *The elastic energy caused by the Earth's rotation and its variation*

This energy is determined by equation (45):

$$E_{\mathrm{R}} = e_2\frac{\omega^4}{9}. \tag{59}$$

For $e_2 = 2.325 \times 10^{50}$ c.g.s. and $e_2 = 0.731 \times 10^{50}$ c.g.s. [10] and the angular velocity of the Earth given by $\omega = \omega_0$ we obtain the following corresponding results:

$$\begin{aligned} E_{\mathrm{R}} &= 0.7305 \times 10^{33}\,\text{c.g.s.} = 0.7305 \times 10^{26}\,\text{Dj} \\ E_{\mathrm{R}} &= 0.2295 \times 10^{33}\,\text{c.g.s.} = 0.2295 \times 10^{26}\,\text{Dj}. \end{aligned} \tag{60}$$

The variation in the elastic energy (59) and (60) is determined by the variation $\delta\omega$ in the Earth's angular velocity:

$$\delta E_{\mathrm{R}} = 4e_2 \frac{\omega_0^4}{9} \frac{\delta\omega}{\omega_0} = 4E_{\mathrm{R}} \frac{\delta\omega}{\omega_0}. \tag{61}$$

Here $\delta\omega$ is the sum of tidal and non-tidal variations in the angular velocity and, in accordance with the evaluation (60), we obtain

$$\delta E_{\mathrm{R}} = 2.922 \times 10^{33} \left[\left(\frac{\delta\omega}{\omega_0} \right)_{\mathrm{t}} + \left(\frac{\delta\omega}{\omega_0} \right)_{\mathrm{nt}} \right] \text{ c.g.s.} \tag{62}$$

Taking into account that relative variations in the angular velocity reach a value of the order of $\delta\omega/\omega_0 \approx 10^{-8} - 10^{-10}$, we can conclude that the variation (62) can be about $\delta E_R = 10^{23} - 10^{24}$ c.g.s., and below we show that the variations in the mutual component of the elastic energy caused by rotational deformation and lunisolar tides are more significant.

Remark Evaluations of the powers connected with global rotational deformation have a formal character here. In reality, in the present epoch we cannot observe this combination of deformations. As a result of our own evolution the elastic rotational energy has disappeared, but the finer effects of interaction and superposition of deformations caused by the variations in the Earth's rotation of course are real and must be studied.

4.3 *The elastic energy caused by the mutual effects of the rotational tide and lunisolar tides*

These mutual terms in accordance with the general formula (45) are determined in the following form:

$$E_{\mathrm{RP}} = E_{\mathrm{RM}} + E_{\mathrm{RS}}, \tag{63}$$

$$E_{\mathrm{RM}} = 2(E_{\mathrm{R}} E_{\mathrm{M}})^{1/2} \left(\frac{a_{\mathrm{M}}}{r_{\mathrm{M}}} \right)^3 P_2(\cos\gamma_{\mathrm{M}}), \quad E_{\mathrm{RS}} = 2(E_{\mathrm{R}} E_{\mathrm{S}})^{1/2} \left(\frac{a_{\mathrm{E}}}{r_{\mathrm{E}}} \right)^3 P_2(\cos\gamma_{\mathrm{S}}). \tag{64}$$

The elastic energies E_{M}, E_{S} and E_{R} are determined by equations (49), (53) and (59).

The approximate equations (64) are obtained from the unperturbed energy values (49) and (53) and from their numerical values (54):

$$\begin{aligned} E_{\mathrm{RM}} &= 2(E_{\mathrm{R}}^{(0)} E_{\mathrm{M}}^{(0)})^{1/2} \left(\frac{a_{\mathrm{M}}}{r_{\mathrm{M}}} \right)^3 P_2(\cos\gamma_{\mathrm{M}}) = 2.5606 \times 10^{28} \text{ c.g.s.} \left(\frac{a_{\mathrm{M}}}{r_{\mathrm{M}}} \right)^3 P_2(\cos\gamma_{\mathrm{M}}), \\ E_{\mathrm{RS}} &= 2(E_{\mathrm{R}}^{(0)} E_{\mathrm{S}}^{(0)})^{1/2} \left(\frac{a_{\mathrm{E}}}{r_{\mathrm{E}}} \right)^3 P_2(\cos\gamma_{\mathrm{S}}) = 1.1729 \times 10^{28} \text{ c.g.s.} \left(\frac{a_{\mathrm{E}}}{r_{\mathrm{E}}} \right)^3 P_2(\cos\gamma_{\mathrm{S}}). \end{aligned} \tag{65}$$

Finally for the discussed terms of the elastic energy we obtain the following expression:

$$\begin{aligned} E_{\mathrm{RM+RS}} = 1.4765 \times 10^{28} \Bigg\{ & 1.7343 \text{ c.g.s.} \left[\left(\frac{a^*}{r^*} \right)^3 P_2(\sin\delta^*) \right]_{\mathrm{Moon}} \\ & + 0.7944 \left[\left(\frac{a^*}{r^*} \right)^3 P_2(\sin\delta^*) \right]_{\mathrm{Sun}} \Bigg\}. \end{aligned} \tag{66}$$

Also for the tidal variation in the angular velocity of the Earth caused by lunar and solar tides (by second harmonics) we have a similar equation:

$$\left(\frac{\delta\omega}{\omega_0}\right)_{\mathrm{t}} = 10^{-8}\left\{1.7343\left[\left(\frac{a^*}{r^*}\right)^3 P_2(\sin\delta^*)\right]_{\mathrm{Moon}} + 0.7944\left[\left(\frac{a^*}{r^*}\right)^3 P_2(\sin\delta^*)\right]_{\mathrm{Sun}}\right\}. \tag{67}$$

This means that for the elastic energy variations (lunisolar and rotational) we can give a simple representation:

$$E_{\mathrm{RM+RS}} = 1.4765 \times 10^{36}\ \text{c.g.s.}\left(\frac{\delta\omega}{\omega_0}\right)_{\mathrm{t}}, \tag{68}$$

$$\delta E_{\mathrm{RM+RS}} = 2.560\,69 \times 10^{28}\ \text{c.g.s.}\left\{\left[\left(\frac{a^*}{r^*}\right)^3 P_2(\sin\delta^*)\right]_{\mathrm{Moon}} + 0.458\,05\left[\left(\frac{a^*}{r^*}\right)^3 P_2(\sin\delta^*)\right]_{\mathrm{Sun}}\right\}, \tag{69}$$

The evaluations performed show that the components of the elastic energy (68) and (69) are more significant and determine the stimulation and activation of the Earth.

The temporal behaviour of this elastic energy for the model of the Earth is analysed graphically. Later, in figure 5, graphs of the elastic energy (69) of the Earth for 1995–2005 are presented. The values of the elastic energy are given in conditional units (1 unit = 1.4765×10^{27} c.g.s.).

5. The dates of the extreme values of elastic energy and their correlations with the dates of large earthquakes

5.1 *The dates of the extreme values of elastic energy in the period 1900–2100*

In figure 2 the graphs of the temporal dependence of the main component of the elastic energy (69) for the long period 1890–2010 is presented. The elastic energy is given in conditional units (1 unit = 1.4765×10^{27} c.g.s.). The decades of years are shown along the horizontal axis.

5.1.1 Cyclicity of the 'tops of trees'. The structure of the graph presents a system of 'trees with roots' . The 'tops of the trees' have a period of about 18.6 years, and the 'roots of the trees' have a period of 4.45 years along the horizontal axis. The 'tops of the trees' reflect the global increase in the planetary tension of the rotating Earth under the mutual gravitational action of the Moon and the Sun. These extremes occur with the period of motion of the nodes of the lunar perturbed orbit. The maximum values of energy (on the red graph) correspond to the passage of the Moon through the equinox of the date. These variations can be approximated by the some average curve which is presented in the top part of figure 2(a) (red curve). We have calculated these variations for an ideal elastic Earth (here we do not take into account the dissipation of the elastic energy on the long timescale). They are significant and probably play an important role in the geodynamic and geophysical planetary processes on the Earth.

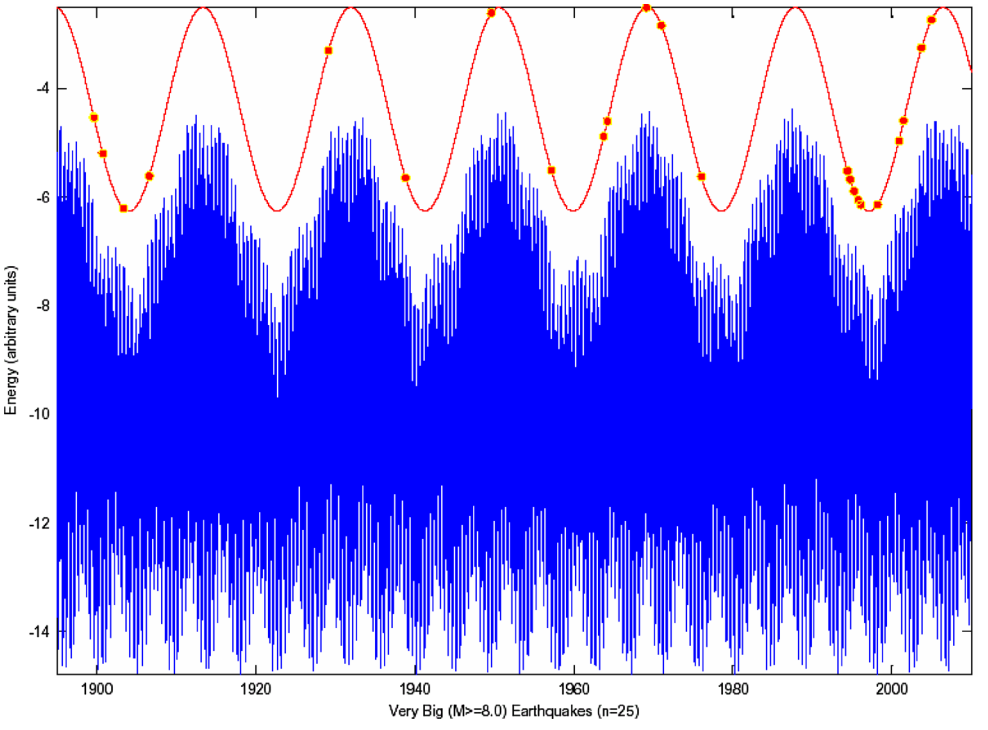

Figure 2. Variations $\delta E_{\mathrm{RM+RS}}$ in the elastic energy in the years 1890–2010 (the 'trees') and graphs of the average values of the elastic energy at (a) the 'tops of the trees' and (b) the 'roots of the trees', with the positions of 25 great earthquakes of magnitude $M \geqslant 8.0$.

We believe that the above-mentioned variations in the Earth's state not only determine the mechanical changes in the Earth's shells but also cause cyclic and synchronous perturbations in all geophysical processes including variations in the physical fields, and perturbations and corresponding changes in the biosphere and noosphere. Our hypothesis is that the extreme values of elastic energy are more difficult for nature and society in our life. We expect that they determine the dates of the largest catastrophes such as large quakes, volcanic eruptions, atmospheric circulations and ecological catastrophes. These extreme dates can be calculated on the basis of the known theories of the orbital motions of the Moon and the Sun.

In table A2 (appendix A) the dates (years) that the 'tops of the trees' form are presented for the last 2000 years (i.e. the period 100–2100). These dates can be used for an analysis of the history of all the catastrophic events in the life of the Earth (earthquakes, volcanoes, climate variations, atmospheric behaviour, etc.), and biosphere and society catastrophes.

5.1.2 Repeated sharp decrease in the elastic energy (the 'roots of the trees'). On the other hand, the 'roots of the trees' in figures 2(a) and (b) reflect another phenomenon. In definite periods of time the Earth produces a periodically active sharp decrease in the elastic energy. These periods are repeated sufficiently frequently (with a period of about 4.45 years). In these states of low elastic energy the Earth is most subject to every type of possible failure and decreases in the stored energy. In particular the seismic elastic energy stored in definite regions of the Earth can be realized in a large earthquake. The last phenomenon is evidently illustrated in figure 2(b) (the green curve at the bottom of the figure) where it is clearly visible that the dates of 17 large quakes in the period 1890–2005 (from the list of 25 great earthquakes,

given in table 1 later) are situated close to the extremes of the graph showing the 'roots of the trees' (i.e. close to the dates of the extreme values of the average elastic energy). This green curve illustrates the average variation in the elastic energy. On the model graph the larger earthquakes in this period (of magnitude greater then 8.0; 25 events) are indicated as red full circles.

5.2 *Repeatability and the expected periodicities in the temporal distribution of the quake events*

On figures 2 and 3 we can see also sufficiently clearly that some series of quakes are situated approximately along concrete horizontal lines. They illustrate an important phenomenon of repeatability of big earthquakes with base periods 18.6 yr and 4.45 yr and with commensurable periods k 18.6 yr and k 4.45 yr ($k = 1, 2, 3, 4, \ldots$). Discovered property of big quakes temporal repetition is very important and let us to give some prognoses on the future about dates of possible big quakes.

5.3 *Intensive increases in the seismic activity in the last 15 years*

A more detailed illustration of the elastic energy curves is given in figure 4 where the phenomenon of the increasing amplitudes of the monthly variations in the elastic energy (69) in the period 1991–2006 is illustrated. With a definite cyclicity and rhythms, the maxima of the variations increase, starting approximately since 1998.

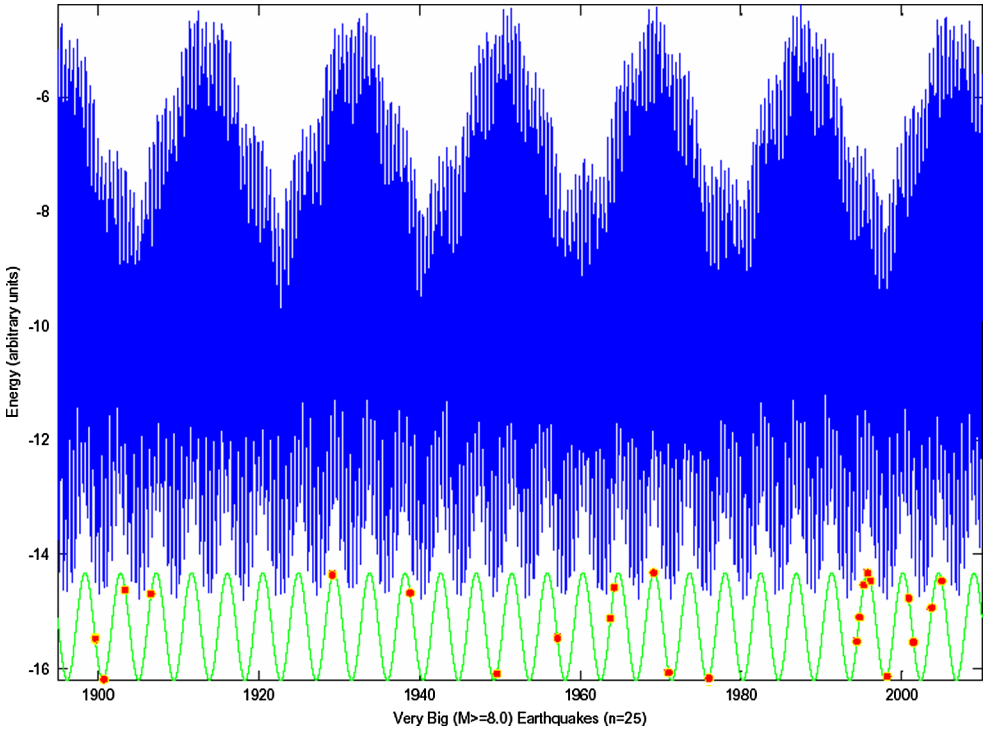

Figure 3. Combination of two long-period graphs from figures 2(a) and (b).

In figure 4 the earthquakes of magnitudes greater than 7.0 are illustrated as yellow full circles with a red periphery. At first sight it seems that the distribution of these points is random but, in fact, we shall show below (see section 5.5) that a definite concentration of quake events has been observed about the dates of the extreme values and the same mean value of the elastic energy if we consider the fine structure of this curve, taking into account its monthly variations. This means that the seismic process (large quakes of magnitude 7.0) are controlled and directed by the Moon and the Sun. Figure 4 also clearly illustrates the phenomenon of the concentration of large quakes in the time interval 1994–2002 (with the centre in 1998). A decrease in the elastic energy is necessary in the middle of this time period, *i.e.* in 1998. Other quakes also correspond to sharp decreases in the elastic energy.

In table 2 of Appendix 1 the dates (day, month, years) of sharp damps are presented for period since 100 till 2100 years. These dates can be used for an analysis of the history of all the catastrophic events in the life of the Earth (earthquakes, volcanoes, climate variations, atmospheric behaviour, etc.), and biosphere and society catastrophes.

The observed phenomena allows us to assume that variations in the elastic energy are connected with seismic activity. Of course, this means that correlation between the orbital motions of the Moon and the Sun and the planetary seismic process really takes place. The variation in the mutual term of the elastic energy (69) is sufficiently large that it significantly controls and dictates the seismic process.

An analysis of the Earth's catastrophes, and the history of the seismic and volcanic events in the depth of the Earth therefore is of great interest here.

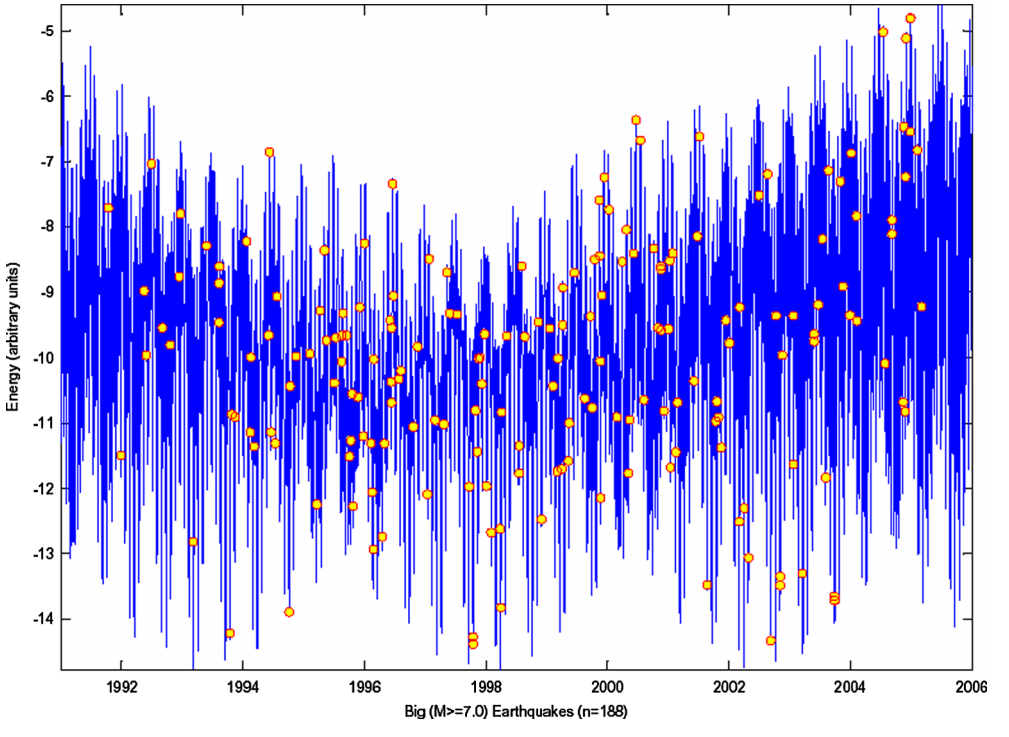

Figure 4. Variations $\delta E_{\mathrm{RM+RS}}$ in the elastic energy in the years 1991–2006 with the positions of 188 large earthquakes of magnitude $M \geqslant 7.0$.

5.4 *Short-period variations in the elastic energy in 1995–2005*

Now we study the temporal variations in the elastic energy on a shorter timescale. Figure 5 shows the annual curves of the elastic energy changes for 1995–2005. All the graphs presented in figure 5 illustrate the variations in the elastic energy in 1995–2005 with periods of perturbed orbital motion of the Moon and the Sun. The main cyclicity here is characterized by the synodic period of the Moon's orbital motion in 28.3 days. The main seismic events of every year (of magnitude greater 7.0) are indicated as yellow full circles with a red periphery on the curves (in this paper, we use data about large earthquakes from the Internet [13]). We can see that a set of events was realized close to the extreme peaks of the graph and close to some mean value of the elastic energy equal to approximately -9.5.

Let us classify the temporal positions of the all events into three groups: I, the first group combines all earthquakes which have occurred near the maximum values of the elastic energy of the appropriate lunar cycle; II, the second group combines all earthquakes which have occurred near the minimum values of the elastic energy of the appropriate lunar cycle; III,

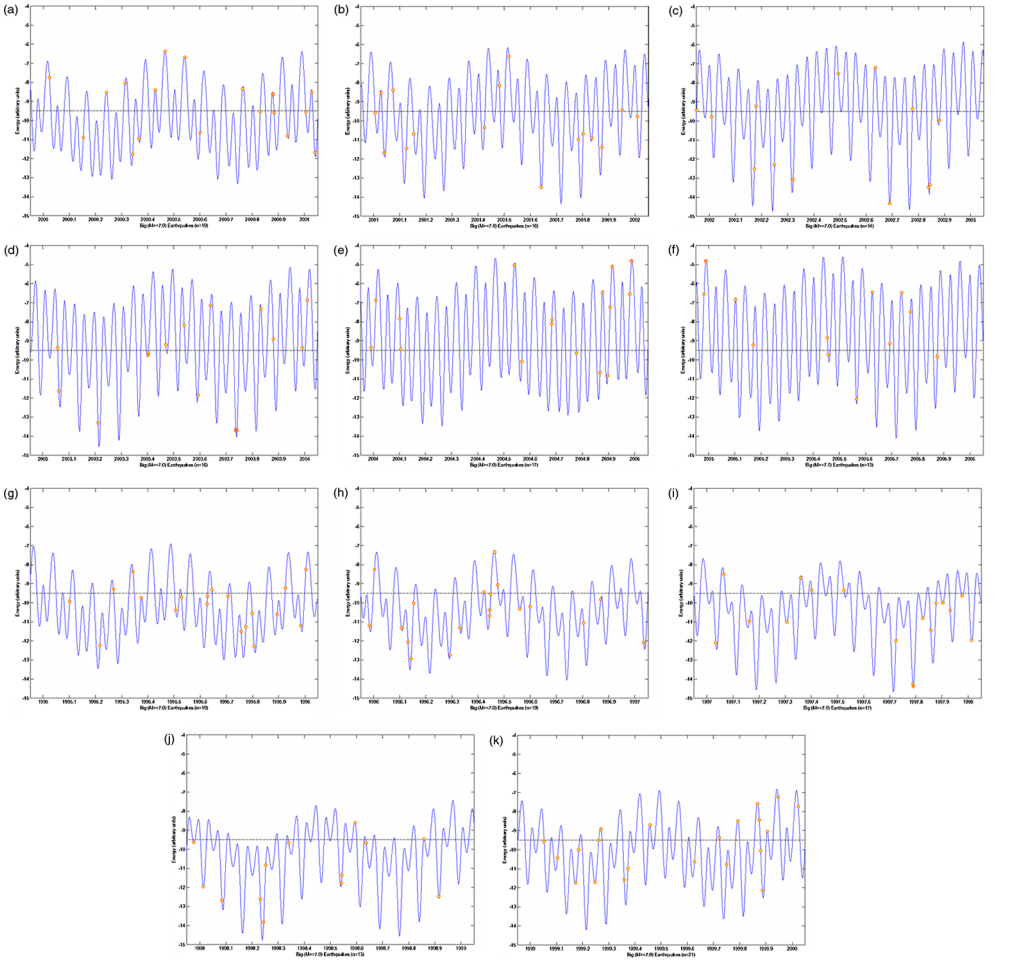

Figure 5. Monthly variations $\delta E_{\mathrm{RM+RS}}$ in the elastic energy with the positions of large earthquakes of magnitude $M \geqslant 7.0$. in (a) 1995, (b) 1996, (c) 1997, (d) 1998, (e) 1999, (f) 2000, (g) 2001, (h) 2002, (i) 2003, (j) 2004 and (k) 2005.

Table 1. Regular distribution of the earthquakes with respect to the extreme values and to the means of the elastic energy.

Year	Number of maxima	Number of minima	Mean	Total number of earthquakes	Number of irregular earthquakes
1995	5	3	4/8	18	6
1996	6	6	2/5	17	3
1997	3	8	0/3	16	5
1998	4	6	1/3	12	1
1999	10	4	1/4	20	5
2000	9	3	2/2	16	2
2001	3	5	2/2	15	5
2002	3	5	2/4	13	3
2003	2	10	1/5	15	2
2004	6	3	2/3	16	5
2005	4	3	3/5	10	0
Sum	55	56	20/44	168	37
Percentage	32.7	33.3	11.9	100	22.0

the third group combines all earthquakes which have occurred near the intermediate values corresponding to elastic energy values equal to -9.5. Each earthquake will be included in the group if its representative point is similar to the nearest extreme point or the average value at a distance of a fifth of the corresponding shoulder of the curve of elastic energy (this distance is calculated and estimated approximately along this curve). The results of the analysis of the grouping of earthquakes are presented in table 1 for every year in the period 1995–2005.

From table 1 it follows that only every fifth large quake has an irregular position. 131 quakes, on the other hand, are characterized by regular positions with respect to the extreme values of the elastic energy curve and to the mean of -9.5. The results obtained here confirm the correlation of the seismic planetary process on the Earth with the orbital motions of the Moon and the Sun.

5.5 *Correlations of the extreme value of the elastic energy and their correlations with the dates of large earthquakes in 2003–2005*

5.5.1 A correlation of the dates of large quakes and the dates of the extreme value of the elastic energy in 2003. Of course, earthquakes are not observed for all the above-mentioned extreme tidal variations (figure 5). Probably this is caused by the process of accumulation of seismic energy. However, in any case, we can predict in a definite statistical sense the dates of future large earthquakes as dates of potential large catastrophes. As a result of the analysis of the theoretical curves of the components of the elastic energy (69) we have determined the dates of possible large earthquakes in 2003. These dates are listed in table 2.

As a result of the analysis of the dates of the 15 largest earthquakes in 2003 of magnitude greater than 7.0, ten earthquakes were observed to correlate with the corresponding dates of the extreme values of the elastic energy (69). Let us list these earthquakes.

The great earthquake in Hokkaido (Japan) of magnitude 8.3 took place on 25 September 2003 at about 20 h, which is close to the date of the extreme value of the elastic energy, 26 September 2003 (18 h). The difference between the times is 22 h. Another parallel earthquake in Hokkaido of magnitude 7.4 occurred on 25 September at about 21 h, which is also close to the same date of the extreme value of the elastic energy, 26 September (18 h). The difference between the times is 21 h. A third large earthquake in this series happened in southwestern Siberia (Russia). It had a magnitude of 7.3 and took place on 27 September at about 11.5 h, which is close to the same date of the extreme value of the elastic energy, 26 September (18 h).

Table 2. The dates of possible large earthquakes in 2003.

Month	Date (time)
January	2 (21 h), 9 (12 h), 16 (19 h), 23 (16 h), 30 (3 h)
February	5 (19 h), 13 (2 h), 19 (21 h), 26 (9 h)
March	5 (1 h), 12 (13 h), 19 (8 h), 25 (17 h)
April	1 (7 h), 8 (23 h), 15 (22 h), 22 (2 h), 28 (12 h)
May	6 (7 h), 13 (12 h), 19 (10 h), 25 (16 h)
June	2 (13 h), 9 (21 h), 15 (1 h), 21 (21 h), 29 (17 h)
July	7 (2 h), 13 (1 h), 19 (4 h), 26 (22 h)
August	3 (4 h), 9 (7 h), 15 (13 h), 23 (5 h), 30 (8 h)
September	5 (14 h), 11 (22 h), 19 (15 h), 26 (18 h)
October	2 (21 h), 9 (5 h), 17 (1 h), 24 (8 h), 30 (6 h)
November	5 (10 h), 13 (9 h), 20 (22 h), 26 (14 h)
December	2 (12 h), 10 (14 h), 18 (8 h), 23 (23 h), 29 (17 h)

In this case the difference between the times is 15.5 h. In other words the dates of the three greatest earthquakes in Asia in 2003 correlate with the date of the extreme value of the elastic energy of the Earth (with its perturbed state).

An earthquake off the east coast of Honshu (Japan) of magnitude 7.0 occurred on 31 October 2003 at about 1 h, which is close to the date of the extreme value of the elastic energy, 30 October 2003 (6 h). The difference between the times is only 19 h. Another earthquake of magnitude 7.0 took place on 26 May at 9.5 h near the east coast of Honshu (Japan). This date is close to the date of the extreme value of the elastic energy, 25 May (16 h) (table 2). The difference between the correlated times is 17.5 h. A large earthquake in the region of the Scotia Sea of magnitude 7.5 happened on 4 August at about 4.5 h, which is related to the date of the extreme value of the elastic energy, 3 August (4 h). The difference between the corresponding times is 24.5 h. An earthquake in the region of Halmahera (Indonesia) of magnitude 7.0 took place on 26 November at about 19.5 h, which is close to the date of the extreme value of the elastic energy, 25 November (16 h). The difference in the times is 27.5 h.

Note also the earthquake in offshore Colima (Mexico) of magnitude 7.6 which happened on 22 January 2003 at about 2 h, which is close to the date of the extreme value of the elastic energy, 23 January (16 h). The difference in the times in this case is 38 h. An earthquake in Amazonas (Brazil) of magnitude 7.1 took place on 20 June at about 6.5 h, which is close to the date of the extreme elastic energy value, 21 June (21 h). The difference in the times is 38.5 h (about 1.5 days). A parallel earthquake on South Island, New Zealand, of magnitude 7.2 occurred on 21 August at about 12 h, which is close to the same date of the extreme value of the elastic energy, 23 August (5 h). The difference in the times is remarkable here, 41 h.

It is worth remarking that the above-mentioned dates in general differ from the dates of the extreme values of variation in another component of the elastic energy (50) studied in [4].

5.5.1.1 Prediction of the dates of Japan quakes in September 2003; the very large earthquake with $M = 8.3$. The date of the real Japan quake on 25 September 2003 (at 19:50:06 coordinated universal time (UTC)) of very large magnitude $M = 8.3$ is close to the date of the extreme value from table 2, 26 September (18 h). In our previous studies and electronic publications [2, 4] we pointed out that a large earthquake would occur on 26.1 September 2003. This conclusion was obtained as a result of the analysis of the component of the elastic energy (50). This phenomenal earthquake took place on Hokkaido island with the epicentre location at 41° 78 N, 143° 86 E, and at a depth of 27 km. This earthquake was accompanied by a tsunami with an estimated wave height of 4.0 m along the southeastern cost of Hokkaido. At least 589 people were injured, extensive damage, landslides and power

outages occurred, and many roads were damaged in southeastern Hokkaido. This earthquake was felt strongly in much of Hokkaido [13].

A second Japan quake on 25 September 2003 with $M = 7.0$ was closer to the predicted date of the large earthquake. It took place on 25 September (at 21:08 UTC) with a large magnitude $M = 7.0$ at Hokkaido island. The epicentre coordinates were 41° 81 N, 143° 51 E, and the depth was 33 km.

Previous extremely large earthquakes in this region ocurred on 4 March 1952 ($M = 8.1$), 16 May 1968 ($M = 7.9$) and 15 January 1993 ($M = 7.6$). The last large earthquake (of magnitude 8 or greater) in the world had a magnitude of 8.4 and occurred on 23 June 2001, near the coast of Peru.

5.5.2 A correlation of the dates of large quakes and the dates of the extreme values of the elastic energy in 2004. Table 3 lists the dates of the extreme values of the component of the elastic energy (69) in 2004.

A simple analysis of dates of the largest quakes in 2004 with a magnitude greater than 7.0 (15 events) has shown that six earthquakes demonstrate correlation with the corresponding dates of the extreme values of the elastic energy (table 3) (including the very large Sumatra quake). In reality the phenomenal earthquake off the west coast of northern Sumatra of magnitude 9.0 took place on 26 December 2004 at about 1 h, which is close to the date of the extreme value of the elastic energy, 26 December (14 h) (see table 3). The difference between the predicted time of the quake (the time when the extreme value of the elastic energy occurs) and the time of the earthquake is only 13 h. A parallel earthquake on Nicobar Islands (India region) of magnitude 7.1 also took place on 26 December at about 4.5 h, which is close to the same date of the extreme value of the elastic energy, 26 December (14 h). The difference between the times is 9.5 h [6, 7].

An earthquake near the west coast of Colombia of magnitude 7.2 ocurred on 15 November 2004 at 9 h. This date is close to the date of the extreme value of the elastic energy, 15 November (17 h) (table 3). The difference between the times is only 8 h. An earthquake in the Fiji region of magnitude 7.1 took place on 15 July at about 4 h, which is very close to the date of the extreme value of the elastic energy, 15 July (19 h). The difference between the corresponding dates is 15 h. A Hokkaido (Japan) quake of magnitude 7.0 took place on 28 November at about 18.5 h, which is close to the date of the extreme value of the elastic energy, 29 November (11 h). The difference between these times is 17.5 h. An earthquake off the west coast of South Island, New Zealand, of magnitude 7.1 occurred on 22 November at about 20 h, which is close to the

Table 3. The dates of the extreme values of the elastic energy of the Earth in 2004.

Month	Date (time)
January	6 (18 h), 14 (11 h), 20 (6 h), 26 (2 h)
February	2 (23 h), 10 (12 h), 16 (13 h), 22 (13 h)
March	1 (8 h), 8 (18 h), 14 (21 h), 20 (23 h), 28 (18 h)
April	5 (4 h), 11 (4 h), 17 (6 h), 25 (4 h)
May	2 (18 h), 8 (12 h), 14 (10 h), 22 (11 h), 30 (6 h)
June	4 (20 h), 10 (13 h), 18 (15 h), 26 (15 h)
July	2 (4 h), 7 (18 h), 15 (19 h), 23 (18 h), 29 (11 h)
August	4 (4 h), 12 (0 h), 19 (19 h), 25 (19 h), 31 (16 h)
September	8 (9 h), 16 (0 h), 22 (2 h), 28 (3 h)
October	5 (18 h), 13 (10 h), 19 (10 h), 25 (11 h)
November	2 (4 h), 9 (23 h), 15 (17 h), 21 (14 h), 29 (11 h)
December	7 (11 h), 13 (1 h), 18 (17 h), 26 (14 h)

date of the extreme value of the elastic energy, 21 November (14 h). The difference between the times is 30 h.

5.5.3 A correlation of the dates of large quakes and the dates of the extreme values of the elastic energy in 2005. The dates of the extreme values of the elastic energy of the Earth for 2005 are given in table 4.

The dates of six earthquakes (out of ten earthquakes) of magnitude greater than 7.0 which occurred in 2005 (before November) demonstrate correlations with the corresponding dates of the extreme values of the elastic energy. An earthquake of magnitude 7.3 in the Honshu (Japan) region took place on 16 August 2005 at about 3 h, which is very close to the date of the extreme value of the elastic energy, 15 August (23 h). The difference between the times is only 4 h. An earthquake of magnitude 7.1 in the Celebes Sea region occurred on 5 February at 12 h, which is very close to the date of the extreme value of the elastic energy, 5 February (18 h). The difference between the times is only 6 h.

An earthquake in the region of the Nicobar Islands (India region) of magnitude 7.3 occurred on 24 July 2005 at about 16 h, which is very close to the date of the extreme value of the elastic energy, 25 July (7 h). The difference between these times is 15 h. Another earthquake of magnitude 7.5 happened on 26 September at about 2 h in the region of northern Peru. This date is close to the date of the extreme value of the elastic energy, 25 September (10 h). The difference between the times is 16 h.

Two other earthquakes should be noted. The first of these took place on 15 June 2005 at 3 h in northern California and had a magnitude of 7.0. This date differs from the date of the extreme value of elastic energy (16 June (11 h)) by 32 h. The second of these was an earthquake in Pakistan of magnitude 7.6 on 8 October at about 4 h, which is close to the date of the extreme value of the elastic energy, 9 October (15 h). The difference between the times is 35 h.

For November 2005 and December 2005 and for the whole of 2006 the possible dates of large earthquakes are specified from the data on the dates of the extreme values of the elastic energy in tables 4 and 5 respectively.

5.5.4 The dates of the extreme value of the elastic energy in 2006. These dates are listed in table 5.

Table 4. The dates of the extreme values of the elastic energy of the Earth in 2005.

Month	Date (time)
January	3 (18 h) , 9 (9 h) , 14 (23 h) , 22 (18 h) , 30 (20 h)
February	5 (18 h) , 11 (10 h) , 19 (1 h) , 26 (22 h)
March	5 (2 h) , 11 (0,h) , 18 (10 h) , 26 (4 h)
April	1 (9 h) , 7 (11 h) , 14 (21 h) , 22 (14 h) , 28 (16 h)
May	4 (18 h) , 12 (5 h) , 20 (1 h) , 25 (23 h) , 31 (21 h)
June	8 (11 h) , 16 (11 h) , 22 (7 h) , 28 (0 h)
July	5 (15 h) , 13 (17 h) , 19 (15 h) , 25 (7 h)
August	1 (19 h) , 9 (19 h) , 15 (23 h) , 21 (18 h) , 29 (1 h)
September	5 (22 h) , 12 (7 h) , 18 (8 h) , 25 (10 h)
October	3 (3 h) , 9 (15 h) , 15 (20 h) , 22 (20 h) , 30 (12 h)
November	5 (22 h) , 12 (3 h) , 19 (5 h) , 26 (22 h)
December	3 (4 h) , 9 (6 h) , 16 (11 h) , 24 (6 h) , 30 (11 h)

Table 5. The dates of the extreme values of the elastic energy of the Earth in 2006.

Month	Date (time)
January	5 (9 h) , 12 (14 h) , 20 (11 h) , 26 (19 h)
February	1 (17 h) , 8 (20 h) , 16 (14 h) , 23 (4 h)
March	1 (5 h) , 8 (3 h) , 15 (18 h) , 22 (13 h) , 28 (20 h)
April	4 (13 h) , 12 (0 h) , 18 (21 h) , 25 (7 h)
May	1 (23 h) , 9 (7 h) , 16 (3 h) , 22 (14 h) , 29 (6 h)
June	5 (14 h) , 12 (8 h) , 18 (16 h) , 25 (12 h)
July	2 (21 h) , 9 (15 h) , 15 (19 h) , 22 (17 h) , 30 (3 h)
August	5 (22 h) , 12 (3 h) , 18 (22 h) , 26 (8 h)
September	2 (8 h) , 8 (15 h) , 15 (5 h) , 22 (12 h) , 29 (16 h)
October	6 (5 h) , 12 (15 h) , 19 (17 h) , 27 (0 h)
November	2 (18 h) , 9 (0 h) , 15 (22 h) , 23 (6 h) , 30 (1 h)
December	6 (8 h) , 13 (4 h) , 20 (11 h) , 27 (3 h)

5.6 *Variations in the Earth's seismic activity in 1998–2004*

Here we shall study the correlation of the times of the earthquakes with the times of the extreme values of the Earth's elastic energy (or its components). Prefiously we have studied the theoretical curves of the change in the elastic energy of lunar-solar deformations of the Earth's mantle and terrestrial-solar deformations on the Moon in the period 1971–1976 [4]. It was shown that the times of quakes are usually sufficiently close to the times of the extreme values of the elastic energy caused by the mutual lunar and solar tides of the Earth. The times of large earthquakes (of magnitudes 7 and 8 and greater) and moonquakes in the considered period of time correlate with the times of the elastic energy extremes.

On this basis we can assume that the variations in the elastic energy are connected with seismic activity. Of course, this means that the correlation between the orbital motions of the Moon and the Sun and the planetary seismic process really occurs. The mutual term of the elastic energy is sufficiently large and significantly controls and dictates the seismic process. This seems natural. Some of the elastic energy with every orbital cycle of the Moon (and the Sun) dissipates to inner geodynamic processes.

In this paper we study first the role of other components of the elastic energy, namely the correlation of the dates of the extreme values of the variation $\delta E_{\mathrm{RM+RS}}$ with the dates of large earthquakes. Then we compare the dates of large earthquakes T_σ of magnitude not less than 7.0 with the corresponding closest dates $T_{1\sigma}$ (minimum) and $T_{2\sigma}$ (maximum) of the extreme values of the variation in the elastic energy. As a result we have determined the factors of deviation by means of the formula (table 6)

$$K_\sigma = \min\left\{\frac{T_{2\sigma} - T_\sigma}{T_{2\sigma} - T_{1\sigma}}, \frac{T_\sigma - T_{1\sigma}}{T_{2\sigma} - T_{1\sigma}}\right\}, k_\sigma \in (0, 1),$$

for all the above-mentioned quakes in the period 1998–2004. We take into account 101 large quakes. The regions of the quakes are given in table 6.

A histogram of the distribution of the parameter k in figure 6 reflects the non-random character of the distribution of the above-discussed quakes with respect to the dates of the extremes values of the variations in the elastic energy. Practically this histogram illustrates the dependence of the number of earthquakes on the values of the factors k_σ for various intervals of its value.

From the obtained histogram it follows that about 15% of quakes occur in the first 8.2 h before and after the extreme values of the tidal variation in the angular velocity of the Earth. About 30.7% of large earthquakes happen in a period of 16.4 h before and after the extreme

Table 6. Relative deviations k_σ in the dates T_σ of earthquakes of magnitude M_σ not less than 7.0 in the period 1998–2004 from the dates of the extreme values of elastic energy.

σ	M_σ	T_σ	Year	Region of the quake	$T_{1\sigma}$ (minimum)	$T_{2\sigma}$ (maximum)	k_σ
1	7.5	04.3 January	1998	Loyalty Islands	04.75 January	10.89 January	0.16
2	7.1	30.5 January	1998	Near the coast of northern Chile	22.97 January	1.43 February	0.62
3	8.1	25.1 March	1998	Balleny Islands	20.85 March	27.35 March	0.68
4	7.2	29.8 March	1998	Fiji	27.35 March	04.27 April	0.63
5	7.0	01.8 April	1998	Southern Sumatra, Indonesia	27.35 March	04.27 April	0.64
6	7.5	04.0 May	1998	Southeast of Taiwan	04.60 May	07.12 May	0.49
7	7.0	16.5 July	1998	Santa Cruz Islands	15.28 July	21.45 July	0.40
8	7.0	17.4 July	1998	Near the north coast of New Guinea	15.28 July	21.45 July	0.68
9	7.2	04.8 August	1998	Near the coast of Ecuador	05.18 August	11.75 August	0.12
10	7.1	20.3 August	1998	Bonin Islands	19.90 August	26.40 August	0.12
11	7.0	09.2 November	1998	Banda Sea	02.45 November	08.95 November	0.09
12	7.7	29.6 November	1998	Ceram Sea	22.00 November	29.09 November	0.10
13	7.0	19.2 January	1999	New Ireland	16.92 January	24.67 January	0.58
14	7.3	06.9 February	1999	Santa Cruz Islands	03.27 February	11.98 February	0.84
15	7.1	04.4 March	1999	Celebes Sea	04.46 March	10.50 March	0.03
16	7.4	05.5 April	1999	New Britain	29.68 March	08.50 April	0.56
17	7.1	08.6 April	1999	Eastern Russia-northeastern China border	29.68 March	08.50 April	0.0
18	7.1	10.9 May	1999	New Britain	06.26 May	13.48 May	0.73
19	7.1	16.0 May	1999	New Britain	13.48 May	18.40 May	0.96
20	7.0	15.9 June	1999	Central Mexico	09.84 June	16.41 June	0.17
21	7.6	17.0 August	1999	Turkey	15.9 August	20.60 August	0.44
22	7.7	20.7 September	1999	Taiwan	17.17 September	26.45 September	0.77
23	7.5	30.7 September	1999	Oaxaca, Mexico	26.45 September	01.98 October	0.87
24	7.2	16.4 October	1999	Southern California	16.40 October	24.40 October	0.00
25	7.2	12.7 November	1999	Turkey	11.94 November	20.35 November	0.18
26	7.0	15.2 November	1999	South Indian Ocean	11.94 November	20.35 November	0.79
27	7.0	19.6 November	1999	New Britain	11.94 November	20.35 November	0.18
28	7.5	26.6 November	1999	Vanuatu Islands	20.35 November	26.60 November	0.00
29	7.0	07.0 December	1999	Kodiak Island	01.00 December	09.60 December	0.60
30	7.3	11.8 December	1999	Luzon, Philippines	09.60 December	18.56 December	0.48
31	7.2	08.7 January	2000	Tonga Islands	08.27 January	14.71 January	0.13
32	7.1	25.1 February	2000	Vanuatu Islands	21.73 February	29.40 February	0.87
33	7.6	28.5 March	2000	Volcano Islands, Japan	27.77 March	04.71 April	0.15
34	7.0	23.4 April	2000	Santiago del Estero province, Argentina	17.03 April	25.69 April	0.53
35	7.6	04.2 May	2000	Minahassa peninsula, Sulawesi	02.55 May	08.19 May	0.58
36	7.2	12.8 May	2000	Jujuy province, Argentina	08.19 May	14.14 May	0.46
37	7.9	04.7 June	2000	Southern Sumatra, Indonesia	04.70 June	04.70 June	0.00
38	7.9	18.6 June	2000	South Indian Ocean	09.39 June	19.20 June	0.12
39	7.4	06.3 August	2000	Bonin Islands (Japan) region	03.63 August	11.01 August	0.71
40	7.0	04.7 October	2000	Vanuatu Islands	27.85 September	05.06 October	0.09
41	7.0	29.4 October	2000	New Ireland region	25.98 October	02.06 November	0.84
42	8.0	16.2 November	2000	New Ireland region	16.28 November	22.55 November	0.00
43	7.8	16.3 November	2000	New Ireland region	16.28 November	22.55 November	0.00
44	7.6	17.9 November	2000	New Ireland region	16.28 November	22.55 November	0.51
45	7.0	06.7 December	2000	Turkmenistan	27.95 November	07.40 December	0.13
46	7.5	01.3 January	2001	Mindanao, Philippines	27.14 December	04.30 January	0.66
47	7.1	09.7 January	2001	Vanuatu Islands	04.30 January	10.11 January	0.14
48	7.0	10.7 January	2001	Kodiak Islands region, Alaska	10.11 January	15.24 January	0.22
49	7.7	13.7 January	2001	El Salvador	10.11 January	15.24 January	0.59
50	7.7	26.1 January	2001	India	22.95 January	29.86 January	0.92
51	7.4	13.8 February	2001	Southern Sumatra, Indonesia	12.56 February	18.52 February	0.42
52	7.1	24.3 February	2001	Northern Molucca Sea	18.52 February	28.00 February	0.78
53	7.2	03.1 June	2001	Kermadec Islands, New Zealand	31.10 May	08.18 June	0.88
54	8.4	23.9 June	2001	Near the coast of Peru	22.95 June	28.21 June	0.46
55	7.6	07.4 July	2001	Near the coast of Peru	05.90 July	13.71 July	0.38

(*Continued*)

Table 6. Continued.

σ	M_σ	T_σ	Year	Region of the quake	$T_{1\sigma}$ (minimum)	$T_{2\sigma}$ (maximum)	k_σ
56	7.1	21.3 August	2001	East of North Island, New Zealand	15.76 August	21.81 August	0.17
57	7.0	12.6 October	2001	South of Mariana Islands	08.95 October	16.00 October	0.96
58	7.5	19.2 October	2001	Banda Sea	16.00 October	22.64 October	0.95
59	7.0	31.4 October	2001	New Britain region	30.00 October	06.18 November	0.34
60	7.8	14.4 November	2001	Qinghai-Xinjiang border, China	12.72 November	19.18 November	0.52
61	7.1	12.6 December	2001	South of Australia	09.80 December	16.09 December	0.89
62	7.2	02.7 January	2002	Vanuatu Islands	30.40 December	05.25 January	0.74
63	7.4	03.5 March	2002	Hindu Kush region, Afghanistan	01.80 March	09.27 March	0.46
64	7.5	05.9 March	2002	Mindanao, Philippines	01.80 March	09.27 March	0.91
65	7.1	31.3 March	2002	Taiwan region	28.47 March	04.67 April	0.69
66	7.1	26.7 April	2002	Mariana Islands	25.85 April	02.62 May	0.21
67	7.3	28.7 June	2002	Eastern Russia-northeastern China border	24.95 June	02.74 July	0.86
68	7.7	19.5 August	2002	Fiji region	19.15 August	26.74 August	0.05
69	7.7	19.5 August	2002	South of the Fiji islands	19.15 August	26.74 August	0.05
70	7.6	08.8 September	2002	Near the north coast of New Guinea	02.05 September	09.13 September	0.10
71	7.6	10.5 October	2002	Irian Jaya region, Indonesia	06.50 October	12.45 October	0.67
72	7.4	02.1 November	2002	Northern Sumatra, Indonesia	27.85 October	02.83 November	0.22
73	7.9	03.9 November	2002	Central Alaska	02.83 November	10.30 November	0.30
74	7.3	17.2 November	2002	Northwest of Kuril Islands	16.04 November	23.40 November	0.32
75	7.3	20.4 January	2003	Solomon Islands	17.12 January	23.71 January	0.98
76	7.6	22.1 January	2003	Offshore Colima, Mexico	17.12 January	23.71 January	0.49
77	7.1	17.7 March	2003	Rat Islands, Aleutian Islands, Alaska	12.10 March	19.20 March	0.43
78	7.0	26.4 May	2003	Near the east coast of Honshu, Japan	24.97 May	03.44 June	0.27
79	7.0	26.8 May	2003	Halmahera, Indonesia	24.97 May	03.44 June	0.35
80	7.1	20.3 June	2003	Amazonas, Brazil	15.71 June	21.90 June	0.53
81	7.6	15.9 July	2003	Carsberg Ridge	12.75 July	19.15 July	0.97
82	7.5	04.2 August	2003	Scotia Sea	03.04 August	09.17 August	0.38
83	7.2	21.5 August	2003	South Island, New Zealand	16.05 August	23.37 August	0.51
84	8.3	25.8 September	2003	Hokkaido (Japan) region	19.27 September	26.10 September	0.08
85	7.4	25.9 September	2003	Hokkaido (Japan) region	19.27 September	26.10 September	0.06
86	7.3	27.5 September	2003	Southwestern Siberia, Russia	26.10 September	02.34 October	0.38
87	7.0	31.1 October	2003	Off the east coast of Honshu, Japan	30.30 October	05.38 November	0.21
88	7.8	17.3 November	2003	Rat Islands, Aleutian Islands, Alaska	11.87 November	21.54 November	0.88
89	7.3	27.7 December	2003	Southeast of the Loyalty Islands	23.75 December	28.80 December	0.45
90	7.1	03.7 January	2004	Southeast of the Loyalty Islands	02.09 December	05.60 January	0.91
91	7.0	05.9 February	2004	Papua, Indonesia	03.94 February	10.99 February	0.55
92	7.3	07.1 February	2004	Near the south coast of Papua, Indonesia	03.94 February	10.99 February	0.90
93	7.1	15.2 July	2004	Fiji region	07.65 July	15.57 July	0.10
94	7.3	25.6 July	2004	Southern Sumatra, Indonesia	24.00 July	29.14 July	0.63
95	7.2	05.4 September	2004	Near the south coast of western Honshu, Japan	31.30 August	08.43 September	0.66
96	7.4	05.6 September	2004	Near the south coast of Honshu, Japan	31.30 August	08.43 September	0.62
97	7.5	11.9 November	2004	Kepulauan Alor, Indonesia	10.06 November	15.83 November	0.63
98	7.2	15.4 November	2004	Near the west coast of Colombia	10.06 November	15.83 November	0.16
99	7.1	22.9 November	2004	Off the west coast of South Island, New Zealand	15.83 November	21.07 November	0.00
100	7.1	26.1 November	2004	Papua, Indonesia	21.07 November	28.85 November	0.71
101	7.2	28.8 November	2004	Hokkaido (Japan) region	21.07 November	28.85 November	0.02

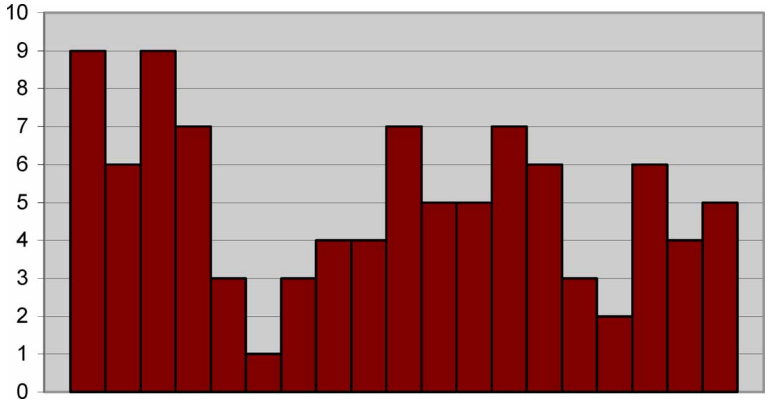

Figure 6. Histogram of earthquakes of magnitude $M > 7.0$ in the period 1998–2004 (the number of events in the time intervals $(T_{\max} - T_{\min})/2n$, $n = 1, 2, 3, 4, 5$).

values. About 35% of quakes take place in a time interval of 32.8–57.4 h (or 1.4–2.4 days) before and after the times of the extreme values of the variation. In both cases there are peaks of concentration of natural events.

Of course, our conclusions are of a preliminary character. Here we have used a rather restricted list of data about large earthquakes (from the last 7 years). Possible tendencies must be studied for longer intervals of time and for fuller basic data about earthquakes, volcanoes and geysers (in the last few centuries).

6. Conclusions

The dates of the extreme values of the elastic energy are very interesting for all-round analysis of the temporal redistribution of the various catastrophic events on the Earth and their possible correlations with the variations in the elastic energy of the Earth. The analysis can involve all the known data about natural processes, ecological catastrophes and also about the biosphere and noosphere processes. Of these, the first to be studied must be large earthquakes, large volcanic eruptions, geyser eruptions, flooding of rivers, periods of droughts and severe atmospheric disturbances (tornadoes, typhoons and large cyclones). The analysis of large fluctuations in the behaviours of physical fields of the Earth (magnetic field, warm ocean currents and others) is also of present interest. We predict also some possible correlations between social, demographic and epidemiological catastrophes, man-made accidents and the extreme values of the variations in the elastic energy determining the general tension state of the full Earth including all its shells. The data given here allow us to carry out important research on the possible correlations between catastrophic historical events in the life of society (wars, revolutions, political conflicts, displays of terrorism, etc.) and the dates of the extreme values of the variations in the general elastic state of the Earth.

This paper is restricted to the analysis of one of the more important components of the elastic energy caused by the mutual combination of the rotational deformations of the mantle and its lunisolar tides. Also we point out that the variations in the elastic energy of the Earth discussed here practically describe the variations in the second harmonics of the force functions of the systems of the axisymetric Earth with the Moon and the Sun (considered as material points). In accordance with Barkin's geodynamical model developed in [14], some of this energy is spent on realizing large endogenous processes. This means that the mechanism of

the shell dynamics (perturbed relative oscillations of the core and mantle) has an influence on the elastic state of the Earth in the same rhythms as the tides studied above. Which of these two mechanism is more effective energetically? This fundamental problem must be studied in future.

Acknowledgements

Acknowledgements Barkin's work was funded by grant SAB2000-0235 from the Secretaria de Estado de Educacion y Universidades) and by grant 02-05-64176 from the Russian Foundation for Basic Research. Partial support of the Spanish research projects AYA-2001-0787 and ESP2001-4533-PE is also acknowledged.

References

[1] Yu.V. Barkin and J.M. Ferrandiz, Astron. Astrophys. Trans. **23** 369 (2004).
[2] Yu.V. Barkin, J.M. Ferrandiz and J.F. Navarro, in *Proceedings of the EGS-AGU-EUG Joint Assembly*, Nice, France, 7–11 April 2003, in Geophys. Res. Abstr. **5** 03227 (2003).
[3] J.M. Ferrandiz, Yu.V. Barkin and J.F. Navarro, in *Proceedings of the Symposium of the IAG Subcommission for Europe 'European Reference Frame EUREF 2003'*, EUREF Publication 13, Vol. 33, Toledo, Spain, 4–7 June 2003 (Verlag des Bundesamtes fur Kartographie und Geodasie, Frankfurkt-am-Main, 2004), pp. 336–341.
[4] Yu.V. Barkin and J.M. Ferrandiz, in *Abstracts of Microsymposium 37 on Comparative Planetology*, Moscow, Russia, 27–29 October 2003 (Vernadsky Institute-Brown University, Moscow, 2003), CD ROM: Topics in Comparative Planetology.
[5] Yu.V. Barkin, J.M. Ferrandiz and J.F. Navarro, in *Proceedings of the Conference on the Evolution of Tectonic Processes in the Earth's History*, Novosibirsk, Russia, 10–13 February 2004 (2004), pp. 41–43 (in Russian), Siberian Department of RAS.
[6] Yu.V. Barkin, J.M. Ferrandiz and M. Garcia Ferrandez, Geophys. Res. Abstr. **7** 07671 (2005).
[7] Yu.V. Barkin, J.M. Ferrandiz and M. Garcia Ferrandez, in *Proceedings of the 36th Annual Lunar and Planetary Science Conference*, in League City, Texas, USA, 14–18 March 2005 (2005), abstract 1076, Houston. Lunar and Planetary Institute.
[8] H. Takeuchi, Trans. Am. Geophys. Union **31** 651 (1950).
[9] J. Getino and J.M. Ferandiz, Celestial Mech. **51** 17 (1991).
[10] J. Getino, Celestial Mech. Dynamics Astron. **53** 11 (1992).
[11] J. Getino, Z. Angew. Math. Phys. **44** 998 (1993).
[12] F. Gilbert and A.M. Dziewonski, Phil. Trans. R. Soc. A **287** 187 (1975).
[13] S. Malone, The Pacific Northwest Seismic Network, Seismosurfing the Internet for earthquake data, http://www.geophys.washington.edu (2004).
[14] Yu.V. Barkin, Izv. Sekzii Nauk Zemle Russ. Akad. Nauk No. 9 45 (2002).

Appendix 1

In the table A1 of Appendix the Julian dates and Calendar dates of the extreme values of elastic energy in 2005 and 2006 years are given (in conditional units with respect to some conditional level). We have named their as crisis days of the Earth as these days the planet is or in the intensive tension state (surplus elastic energy) or is in the weakened state (at dump of excessive elastic energy). These states must be directly reflected in the all natural planetary processes.

In next table A2 the dates of maximums of the curve "trees tops" which can be interpreted as approximating average curve of variations of elastic energy caused by interaction of rotational and orbital luni-solar tides are given.

In the table A3 dates of minimums of the curve "tree roots" for period 100–2100 years are given. These dates correspond to average curve of variations of elastic energy caused by interaction of rotational and orbital luni-solar tides.

These dates present definite interest for all-round analysis of the temporal redistribution of the various catastrophic events on the Earth and their possible correlations with variations

Table A1. Crisis days of the Earth in 2005 and 2006 years. Julian day 1827.0 corresponds to 1.00 January 2005.

	Crisis days of the Earth in 2005 year			Crisis days of the Earth in 2006 year		
Month	Extreme 2005	Julian dates	Calendar dates	Extreme 2006	Julian dates	Calendar dates
January	min −1.299	1829.992	2.992 Jan.	min −2.305	2197.222	05.222 Jan.
	max 3.457	1835.816	8.816 Jan.	max 4.907	2204.507	12.507 Jan.
	min −1.956	1841.982	14.982 Jan.	min −0.547	2212.213	20.213 Jan.
	max 4.780	1849.761	22.761 Jan.	max 3.480	2218.089	26.089 Jan.
	min −1.720	1857.314	30.314 Jan.			
February	max 2.862	1863.071	5.071 Feb.	min −3.215	2224.581	01.581 Feb.
	min −2.912	1869.361	11.361 Feb.	max 4.035	2231.846	08.846 Feb.
	max 3.770	1877.082	19.082 Feb.	min −1.154	2239.470	16.470 Feb.
	min −2.406	1884.563	26.563 Feb.	max 2.793	2245.363	22.363 Feb.
				min −4.139	2251.939	28.939 Feb.
March	max 2.310	1890.403	4.403 Mar.	max 3.141	2259.198	08.198 Mar.
	min −3.553	1896.701	10.701 Mar.	min −1.591	2266.621	15.621 Mar.
	max 3.126	1904.389	18.389 Mar.	max 2.586	2272.708	21.708 Mar.
	min −2.726	1911.787	25.787 Mar.	min −4.356	2279.278	28.278 Mar.
	max 2.296	1917.789	31.789 Mar.			
April	min −3.402	1923.991	6.991 Apr.	max 2.917	2286.517	04.517 Apr.
	max 3.362	1931.668	14.668 Apr.	min −1.451	2293.753	11.753 Apr.
	min −2.357	1939.053	22.053 Apr.	max 3.074	2300.092	18.092 Apr.
	max 2.864	1945.167	28.167 Apr.	min −3.709	2306.599	24.599 Apr.
May	min −2.624	1951.262	4.262 May	max 3.507	2313.778	01.778 May
	max 4.278	1958.925	11.925 May	min −0.803	2320.973	08.973 May
	min −1.543	1966.396	19.396 May	max 3.894	2327.456	15.456 May
	max 3.567	1972.482	25.482 May	min −2.737	2333.913	21.913 May
	min −1.901	1978.555	31.555 May	max 4.398	2341.005	29.005 May
June	max 5.127	1986.188	08.188 Jun.	min −0.137	2348.315	05.315 Jun.
	min −0.895	1993.791	15.791 Jun.	max 4.396	2354.756	11.756 Jun.
	max 3.841	1999.728	21.728 Jun.	min −2.247	2361.235	18.235 Jun.
	min −1.875	2005.892	27.892 Jun.	max 4.840	2368.250	25.250 Jun.
July	max 5.217	2013.480	05.480 Jul.	min 0.029	2375.712	02.712 Jul.
	min −0.874	2021.169	13.169 Jul.	max 4.183	2381.997	08.997 Jul.
	max 3.480	2026.950	18.950 Jul.	min −2.655	2388.573	15.573 Jul.
	min −2.630	2033.262	25.262 Jul.	max 4.450	2395.551	22.551 Jul.
				min −0.401	2403.050	30.050 Jul.
August	max 4.471	2040.805	01.805 Aug.	max 3.448	2409.229	05.229 Aug.
	min −1.415	2048.467	09.467 Aug.	min −3.652	2415.921	11.921 Aug.
	max 2.806	2054.215	15.215 Aug.	max 3.525	2422.905	18.905 Aug.
	min −3.610	2060.630	21.630 Aug.	min −1.027	2430.245	26.245 Aug.
	max 3.483	2068.142	29.142 Aug.			
September	min −1.995	2075.676	05.676 Sep.	max 2.815	2436.510	01.510 Sep.
	max 2.403	2081.554	11.554 Sep.	min −4.447	2443.269	08.269 Sep.
	min −4.062	2087.969	17.969 Sep.	max 2.787	2450.268	15.268 Sep.
	max 3.035	2095.457	25.457 Sep.	min −1.308	2457.319	22.319 Sep.
	max 2.833	2463.860	28.860 Sep.			
October	min −2.075	2102.861	02.861 Oct.	min −4.405	2470.610	05.610 Oct.
	max 2.646	2108.94	08.940 Oct.	max 2.794	2477.588	12.588 Oct.
	min −3.652	2115.276	15.276 Oct.	min −0.996	2484.396	19.396 Oct.
	max 3.466	2122.726	22.726 Oct.	max 3.531	2491.241	26.241 Oct.
	min −1.530	2130.107	30.107 Oct.			
November	max 3.374	2136.311	05.311 Nov.	min −3.564	2497.944	01.944 Nov.
	min −2.745	2142.571	11.571 Nov.	max 3.492	2504.843	08.843 Nov.
	max 4.403	2149.965	18.965 Nov.	min −0.326	2511.603	15.603 Nov.
	min −0.751	2157.449	26.449 Nov.	max 4.369	2518.596	22.596 Nov.
				min −2.603	2525.274	29.274 Nov.
December	max 4.011	2163.619	02.619 Dec.	max 4.274	2532.064	06.064 Dec.
	min −2.110	2169.881	08.881 Dec.	min 0.162	2538.953	12.953 Dec.
	max 5.068	2177.214	16.214 Dec.	max 4.679	2545.889	19.889 Dec.
	min −0.328	2184.848	23.848 Dec.	min −2.298	2552.604	26.604 Dec.
	max 4.050	2190.862	29.862 Dec.			

Table A2. Dates of maximums of approximating average curve of "tops of trees" in period 100–2100 years.

4 December 107	21 June 610	5 January 1113	3 August 1615
15 July 126	30 January 629	18 August 1131	14 March 1634
23 February 145	11 September 647	29 March 1150	24 October 1652
6 October 163	23 April 666	7 November 1168	5 June 1671
17 May 182	2 December 684	20 June 1187	14 January 1690
26 December 200	14 July 703	29 January 1206	27 August 1708
8 August 219	23 February 722	9 September 1224	8 April 1727
19 March 238	4 October 740	22 April 1243	17 November 1745
28 October 256	16 May 759	1 December 1261	29 June 1764
10 June 275	26 December 777	12 July 1280	8 February 1783
19 January 294	6 August 796	22 February 1299	20 September 1801
30 August 312	18 March 815	3 October 1317	2 May 1820
12 April 331	27 October 833	14 May 1336	12 December 1838
21 November 349	8 June 852	25 December 1354	23 July 1857
22 July 368	18 January 871	5 August 1373	4 March 1876
12 February 387	29 August 889	16 March 1392	14 October 1894
23 September 405	10 April 908	27 October 1410	26 May 1913
4 May 424	20 November 926	7 June 1429	6 January 1932
15 December 442	1 July 945	17 January 1448	17 August 1950
26 July 461	11 February 964	29 August 1466	28 March 1969
6 March 480	22 September 982	9 April 1485	8 November 1987
17 October 498	3 May 1001	19 November 1503	19 June 2006
28 May 517	14 December 1019	1 July 1522	28 January 2025
7 January 536	25 July 1038	9 February 1541	10 September 2043
19 August 554	5 March 1057	21 September 1559	21 April 2062
30 March 573	16 October 1075	2 May 1578	30 November 2080
9 November 591	27 May 1094	22 December 1596	13 July 2099

Table A3. Dates of minimums of the approximating average elastic energy on curve of "three roots" (Fig. 3) in period 100–2100 years.

29 October 95	31 January 600	9 May 1104	30 August 1608
1 April 100	4 July 604	11 October 1108	1 February 1613
2 September 104	6 December 608	14 March 1113	6 July 1617
4 February 109	9 May 613	16 August 1117	8 December 1621
9 July 113	11 October 617	18 January 1122	11 May 1626
10 December 117	15 March 622	22 June 1126	13 October 1630
14 May 122	16 August 626	23 November 1130	17 March 1635
15 October 126	18 January 631	27 April 1135	18 August 1639
19 March 131	21 June 635	29 September 1139	20 January 1644
21 August 135	23 November 639	1 March 1144	23 June 1648
22 January 140	26 April 644	3 August 1148	25 November 1652
25 June 144	27 September 648	5 January 1153	28 April 1657
26 November 148	1 March 653	8 June 1157	30 September 1661
30 April 153	3 August 657	10 November 1161	4 March 1666
2 October 157	4 January 662	14 April 1166	5 August 1670
5 March 162	8 June 666	15 September 1170	7 January 1675
7 August 166	10 November 670	17 February 1175	11 June 1679
8 January 171	13 April 675	22 July 1179	13 November 1683
12 June 175	15 September 679	23 December 1183	15 April 1688
14 November 179	17 February 684	26 May 1188	17 September 1692
16 April 184	20 July 688	28 October 1192	19 February 1697
18 September 188	22 December 692	31 March 1197	25 July 1701
19 February 193	25 May 697	2 September 1201	26 December 1705
24 July 197	27 October 701	4 February 1206	30 May 1710
26 December 201	31 March 706	8 July 1210	1 November 1714
29 May 206	1 September 710	10 December 1214	4 April 1719
31 October 210	3 February 715	14 May 1219	6 September 1723
3 April 215	8 July 719	15 October 1223	8 February 1728
5 September 219	9 December 723	18 March 1228	12 July 1732
7 February 224	12 May 728	20 August 1232	13 December 1736

(*Continued*)

Table A3. Continued.

10 July 228	14 October 732	22 January 1237	17 May 1741
12 December 232	17 March 737	25 June 1241	19 October 1745
15 May 237	19 August 741	27 November 1245	22 March 1750
17 October 241	21 January 746	1 May 1250	24 August 1754
21 March 246	24 June 750	2 October 1254	26 January 1759
22 August 250	26 November 754	6 March 1259	30 June 1763
24 January 255	30 April 759	8 August 1263	1 December 1767
27 June 259	1 October 763	9 January 1268	4 May 1772
29 November 263	4 March 768	12 June 1272	6 October 1776
2 May 268	5 August 772	14 November 1276	10 March 1781
3 October 272	7 January 777	17 April 1281	11 August 1785
7 March 277	11 June 781	19 September 1285	13 January 1790
9 August 281	12 November 785	21 February 1290	17 June 1794
10 January 286	16 April 790	25 July 1294	18 November 1798
14 June 290	18 September 794	27 December 1298	23 April 1803
15 November 294	19 February 799	31 May 1303	25 September 1807
19 April 299	24 July 803	2 November 1307	27 February 1812
21 September 303	26 December 807	4 April 1312	30 July 1816
22 February 308	28 May 812	6 September 1316	1 January 1821
26 July 312	30 October 816	8 February 1321	5 June 1825
27 December 316	3 April 821	12 July 1325	7 November 1829
31 May 321	4 September 825	14 December 1329	10 April 1834
2 November 325	6 February 830	18 May 1334	12 September 1838
5 April 330	11 July 834	19 October 1338	14 February 1843
7 September 334	12 December 838	23 March 1343	19 July 1847
9 February 339	16 May 843	25 August 1347	20 December 1851
13 July 343	18 October 847	27 January 1352	23 May 1856
15 December 347	20 March 852	29 June 1356	25 October 1860
17 May 352	22 August 856	1 December 1360	28 March 1865
19 October 356	24 January 861	5 May 1365	30 August 1869
23 March 361	27 June 865	6 October 1369	1 February 1874
24 August 365	29 November 869	10 March 1374	6 July 1878
26 January 370	2 May 874	12 August 1378	7 December 1882
29 June 374	4 October 878	13 January 1383	11 May 1887
1 December 378	8 March 883	17 June 1387	13 October 1891
5 May 383	9 August 887	19 November 1391	16 March 1896
6 October 387	11 January 892	21 April 1396	18 August 1900
9 March 392	14 June 896	23 September 1400	20 January 1905
11 August 396	15 November 900	25 February 1405	24 June 1909
12 January 401	19 April 905	30 July 1409	26 November 1913
16 June 405	21 September 909	31 December 1413	29 April 1918
17 November 409	22 February 914	4 June 1418	1 October 1922
21 April 414	27 July 918	6 November 1422	5 March 1927
23 September 418	29 December 922	9 April 1427	7 August 1931
24 February 423	1 June 927	11 September 1431	8 January 1936
29 July 427	3 November 931	13 February 1436	11 June 1940
30 December 431	6 April 936	16 July 1440	13 November 1944
2 June 436	7 September 940	18 December 1444	17 April 1949
4 November 440	9 February 945	22 May 1449	18 September 1953
7 April 445	14 July 949	24 October 1453	20 February 1958
9 September 449	15 December 953	27 March 1458	25 July 1962
11 February 454	19 May 958	29 August 1462	27 December 1966
15 July 458	21 November 962	31 January 1467	30 May 1971
17 December 462	24 March 967	4 July 1471	1 November 1975
20 May 467	26 August 971	6 December 1475	4 April 1980
22 October 471	28 January 976	9 May 1480	5 September 1984
25 March 476	30 June 980	11 October 1484	7 February 1989
26 August 480	2 December 984	14 March 1489	12 July 1993
28 January 485	6 May 989	16 August 1493	14 December 1997
2 July 489	7 October 993	18 January 1498	17 May 2002
3 December 493	11 March 998	21 June 1502	19 October 2006

(*Continued*)

Table A3. Continued.

7 May 498	13 August 1002	23 November 1506	23 March 2011
9 October 502	14 January 1007	27 April 1511	25 August 2015
12 March 507	18 June 1011	28 September 1515	26 January 2020
14 August 511	20 November 1015	1 March 1520	29 June 2024
15 January 516	22 April 1020	3 August 1524	1 December 2028
18 June 520	24 September 1024	5 January 1529	5 May 2033
20 November 524	26 February 1029	8 June 1533	6 October 2037
23 April 529	30 July 1033	10 November 1537	10 March 2042
25 September 533	1 January 1038	14 April 1542	12 August 2046
27 February 538	5 June 1042	15 September 1546	14 January 2051
31 July 542	6 November 1046	17 February 1551	17 June 2055
2 January 547	10 April 1051	22 July 1555	19 November 2059
5 June 551	12 September 1055	24 December 1559	22 April 2064
7 November 555	13 February 1060	26 May 1564	24 September 2068
10 April 560	17 July 1064	28 October 1568	25 February 2073
11 September 564	19 December 1068	1 April 1573	30 July 2077
13 February 569	22 May 1073	2 September 1577	1 January 2082
18 July 573	24 October 1077	4 February 1582	5 June 2086
19 December 577	28 March 1082	19 July 1586	6 November 2090
23 May 582	29 August 1086	21 December 1590	10 April 2095
24 October 586	31 January 1091	24 May 1595	12 September 2099
28 March 591	5 July 1095	26 October 1599	
30 August 595	6 December 1099	29 March 1604	

of elastic energy of the Earth. For analysis can be involved all known data about natural processes, ecology catastrophes and also about biosphere and noosphere processes. From them in first must be studied big earthquakes, grandiose volcanic eruptions, geyser eruptions, flooding floods of the rivers, periods of droughts, atmospheric accidents (tornados, typhoons, the big cyclones). The analysis of big fluctuations in behavior of physical fields of the Earth (magnetic field, warm stream and others) presents important interest. We predict also some possible correlations of social, demographic, epidemiology catastrophes, man-made accidents with extremes of variations of the elastic energy determining of the general tension state of the full Earth including all its shells. The data given here allow to carry out the important research of possible correlations of catastrophic historical events in the life of society (wars, revolutions, political conflicts, displays of terrorism etc.) with variations of the general elastic state of the Earth, its physical fields with dates of extreme states.

Figure A1 illustrates the main tendencies in variations of the full numbers of earthquakes with definite magnitudes (with step 0.5 from 4.0 to 8.5) in last century. The fundamental phenomenon which is presented by figure A1 is the existence of close correlation of the dates of extreme values of elastic energy (approximating curve) of the earth and the dates (periods) of its extreme seismic activity in the last century (for earthquakes with magnitude 8 and 8.5). We can see that the “buildings – skyscrapers” of zones of earthquakes (with amplitudes 8 and 8.5) are marked by vertical arrows corresponding to extreme values of elastic energy of the Earth. It is worth to remark also that all arrows correspond to "roots of trees"from the figure 3 in p. 5.1.2. Exception here can be connected only with two extreme values of elastic energy for dates 1954 and 1967 years (from the full list of 23 dates). It means that predicted dates of seismic activization of the Earth in 21th century from the tables A2 and A3 in reality will correspond in the majority by catastrophic earthquakes in this century with largest magnitudes in 8 and more. In other words practically we approximately know positions of all "seismic skyscrapers"in next century. Unfortunately to them there will correspond the heaviest events in life of the Earth and a society. The dates of future seismic catastrophic activization of the Earth are given in last column of the table A3.

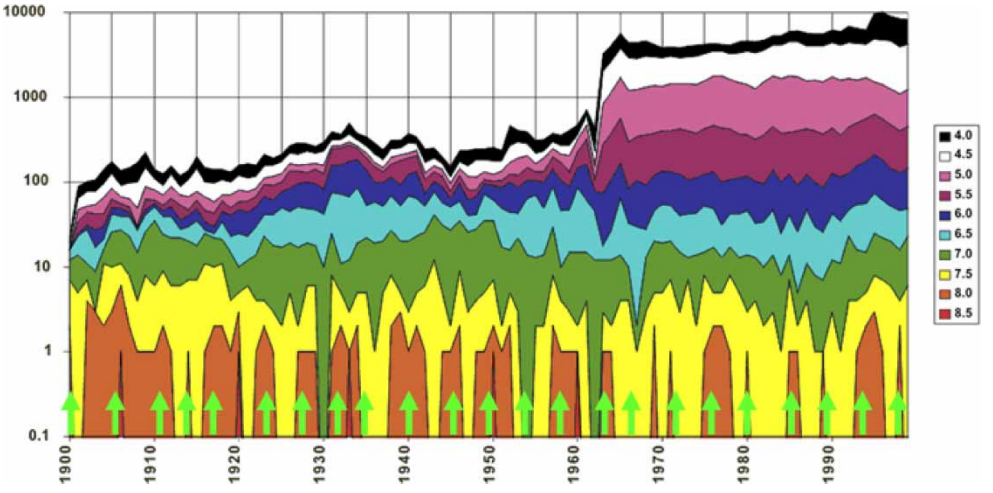

Figure A1. The annual numbers of earthquakes of magnitude 4.0–8.5 in the last century [13]. The positions of the peaks of the extreme values of the elastic energy (arrows). Correlation of 'skyscraper' positions of earthquakes with magnitudes 8.0–8.5 and elastic energy peaks.